Transitions of the 3D Medial Axis Under a One-Parameter Family of Deformations

Peter J. Giblin[†], Benjamin B. Kimia[‡], and Anthony J. Pollitt[†]

Abstract

The instabilities of the medial axis of a shape under deformations have long been recognized as a major obstacle to its use in recognition and other applications. These instabilities, or *transitions*, occur when the structure of the medial axis graph changes abruptly under deformations of shape. The recent classification of these transitions in 2D for the medial axis and for the shock graph was a key factor both in the development of an object recognition system where the classified instabilities were utilized to represent deformation paths. The classification of generic transitions of the 3D medial axis could likewise potentially lead to a similar representation in 3D. In this paper, these transitions are classified, by examining the order of contact of spheres with the surface, leading to an enumeration of possible transitions, which are then examined on a case by case basis. Some cases are ruled out as never occurring in any family of deformations, while others are shown to be non-generic in a one-parameter family of deformations. Finally, the remaining cases are shown to be viable by developing a specific example for each. Our work is inspired by that of Bogaevsky who obtained the transitions as part of an investigation of viscosity solutions of Hamilton-Jacobi equations. Our contribution is to give a more down-to-earth approach, bringing this work to the attention of the computer vision community, and to provide explicit constructions for the various transitions using simple surfaces. We believe that the classification of these transitions is vital to the successful regularization of the medial axis in its use in real applications.

1 Introduction

The practical use of the Medial Axis ($\mathcal{MA}$) in visual tasks such as object recognition, perceptual grouping, shape modeling, shape tracking, *etc*, is adversely affected by the omni-present *instabilities* of the $\mathcal{MA}$ under deformations of shape. This inherent instability of the $\mathcal{MA}$ is illustrated for 2D $\mathcal{MA}$ in Figure 1 and is also prominent in 3D. Previous approaches have either embedded an implicit regularization in the $\mathcal{MA}$ detection process [19, 28] or have explicitly included a post-processing "pruning" mechanism [23, 26]. An alternative to reducing

[†]Dept of Mathematical Sciences, The University of Liverpool, Liverpool, England L69 3BX, pjgiblin@liv.ac.uk

[‡]Division of Engineering, Brown University, Providence, RI, USA, kimia@lems.brown.edu

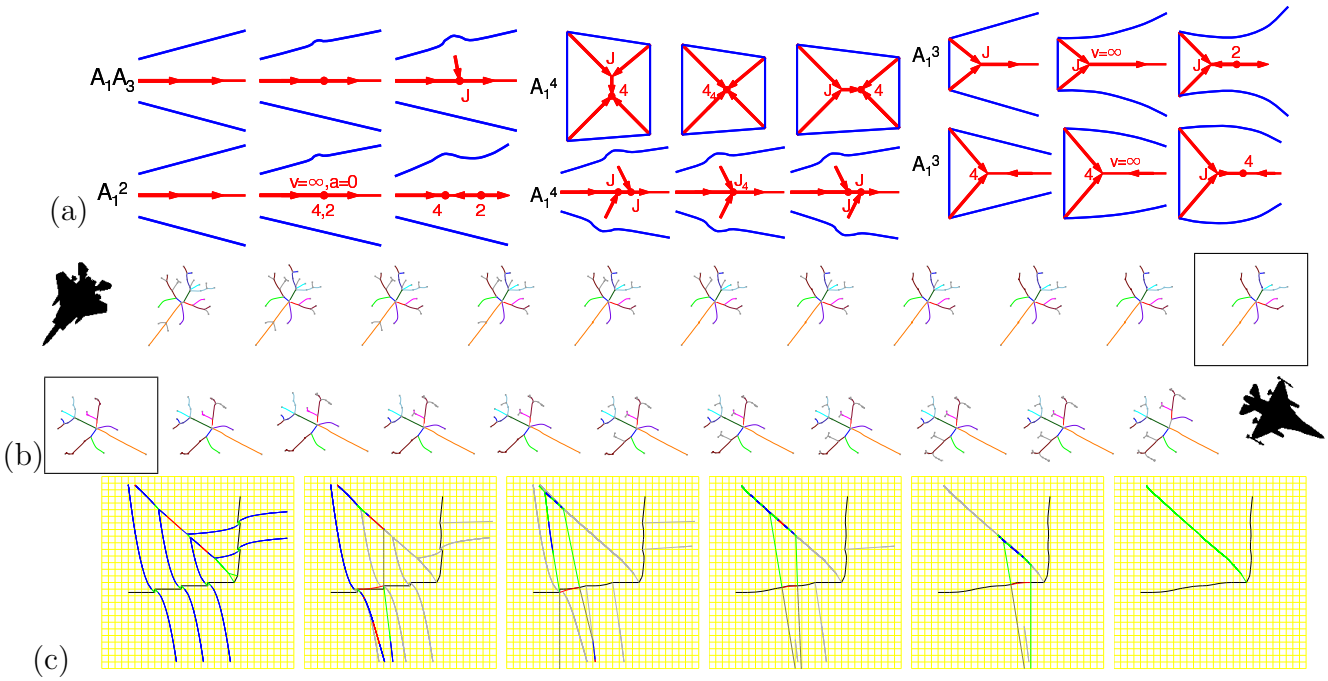

Figure 1: This figure illustrates the importance of $\mathcal{MA}$ transitions for object recognition and shape smoothing. (a) The two instabilities of the $\mathcal{MA}$, namely, the A_1A_3 (*e.g.*, often arising from noise on the boundary) and A_1^4, generalized to six transitions of the shock graph, (b) A deformation path between two shapes is characterized by a sequence of transitions. Sebastian *et al.* [25] search for the geodesic path by searching among all sequences of transitions that bring two shapes' $\mathcal{MA}$ in register, as shown here. (c) The smoothing of noise with blurring discontinuities such as the corner of the L-figure is challenging, but can be achieved through a sequence of transitions, effecting structural smoothing [29].

the effect of the $\mathcal{MA}$ instability is to utilize this instability itself as the key representation of a shape deformation. Sebastian *et al.* [25] use the full classification of the shock graph ($\mathcal{MA}$ endowed with a finer classification based on dynamics of flow) [13]. Specifically, they define shapes with identical shock graph topology as equivalent and observe that paths of deformation between two shapes undergo a distinct set of instabilities or transitions. They define deformation paths having the same transition sequence as equivalent and then develop an edit distance algorithm [17, 18] to search for the geodesic paths, an example of which is shown in Figure 1(b) The cost of this optimal path defines the dissimilarity between two shapes and is used to index into a database of shapes with excellent recognition rates: for a 1032 shape database the recognition rate is 97%, remaining impressively flat in the precision-recall curve [25]. The use of transitions is also significant in shape modeling [30], smoothing shape [29], Figure 1(c) and perceptual grouping [16, 27].

In fact, based on an early version of this paper [12], we have already used this classification

for smoothing shape [21] as shown in Figure 3, and for registration of shapes with different samplings but with overlap [8]. See also an overview of a $\mathcal{MA}$ application in [22] and the recent work of [7].

The transitions of the 2D Medial Axis under a one-parameter family of deformations were derived in [13] using results from transitions of the symmetry set [4]. The former comprise two transitions, as shown in Figure 1a, labeled as A_1A_3 and A_1^4. The notation A_k^n implies k-fold tangency at n places between a circle and the curve being studied (silhouette of a shape), Figure 7. Thus A_1^2 indicates the most generic situation of a circle, centered on the medial axis and tangent at two places each with regular tangency to the curve (that is '1-fold' tangency at each contact point, meaning that each tangency results from the coincidence of exactly *two* intersection points between the circle and curve). Similarly A_1^3 indicates a circle tangent at three places each with regular tangency, and A_3 indicates a circle tangent at a curvature extremum. This is '3-fold' tangency because instead of two coincident intersections between a circle and the curve we have four coincident intersections. The three types A_1^2, A_1^3, and A_3 are the only generic forms of the medial axis in 2D. Similarly, it has been shown that generic transitions under a one-parameter family of deformations are the A_1A_3 (tangency of types A_1 and A_3 at distinct points) and A_1^4 transitions [13]. The A_1A_3 transition occurs frequently due to boundary noise and is recognized as one of the classical instabilities of the medial axis. This transition is the result of formation of a bump on the boundary of the shape which initially bends the medial axis, but when it grows in size it will eventually 'break' the axis leading to the growth of a new branch, Figure 1(a). The second medial axis transition, the A_1^4 transition, occurs when a smooth A_1^2 curve segment on the medial axis between two A_1^3 points shrinks to a point so that the combination of two three-contact A_1^3 points leads to a single four-contact A_1^4 point (this is generic only in a family of curves), Figure 1(a). As the shape is compressed along the direction of the central A_1^2 curve, this curve shrinks so that eventually its A_1^3 end-points overlap, as in the central figure in the top row of Figure 1, the A_1^4 transition. Additional deformations of the shape will form a new A_1^2 axis by swapping the pairing of the four branches coming into the A_1^4 points.

An entirely analogous approach on 3D object recognition, 3D shape smoothing, *etc.* can be developed if the structural instabilities, or the transitions, of the medial axis for 3D shape are classified. The local form of the 3D $\mathcal{MA}$ has already been derived [14] and is summarized below. This paper investigates the transitions of the medial axis in 3D, seven in total, following

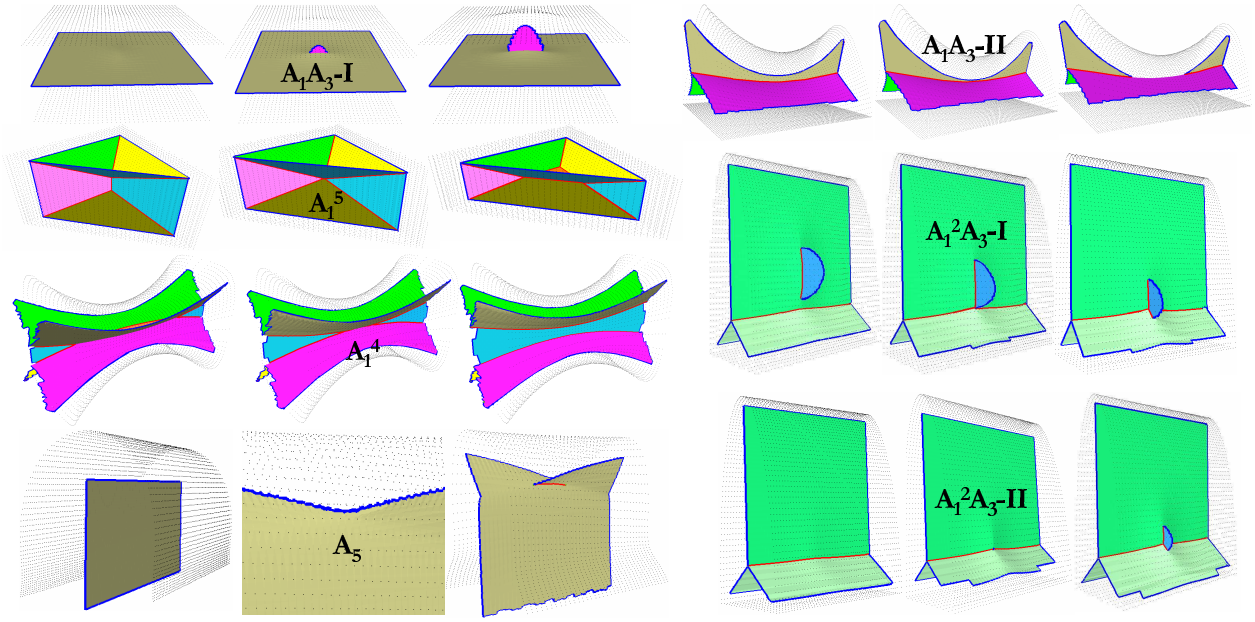

Figure 2: The seven cases of $\mathcal{MA}$ transitions across a one-parameter family of shape deformations.

the work of Bogaevksy on a more general problem [2, 3, 1]. Our contribution is threefold: we derive the transitions by appealing to some general principles of singularity theory and by a close inspection of the geometry of the medial axis; we give an idea of recent practical applications of these results, and we give explicit examples of the transitions for families of surfaces, thereby showing that these transitions do occur in the generic setting. It should be noted that from a geometrical and practical point of view, there are potentially $2 \times 7 = 14$ transitions, since they may take place in either direction. We summarize the contribution of this paper, the classification of $\mathcal{MA}$ transitions in Figure 2. When presented with two 'nearby' medial axes (*e.g.*, obtained from different scans of the same object or closely similar objects) it is important to be able to see transitions which are 'about to happen' in either direction. The paper is organized as follows. First we describe the 3D local form of the $\mathcal{MA}$ and give an overview of how the classifications of the transitions of the 3D $\mathcal{MA}$ are obtained in Section 2. In Section 3 we present a geometric view of how the transition of the $\mathcal{MA}$ can arise from collision of $\mathcal{MA}$ points, curves, and surfaces. In Section 4, we relate this approach to the work of Bogaevsky. In Section 5 we show that each of the $\mathcal{MA}$ transition in fact does occur by constructing an example for each and also simulating the transition process. Section 6 conclude the paper.

Recently James Damon has highlighted the importance of the transitions on the 3D medial

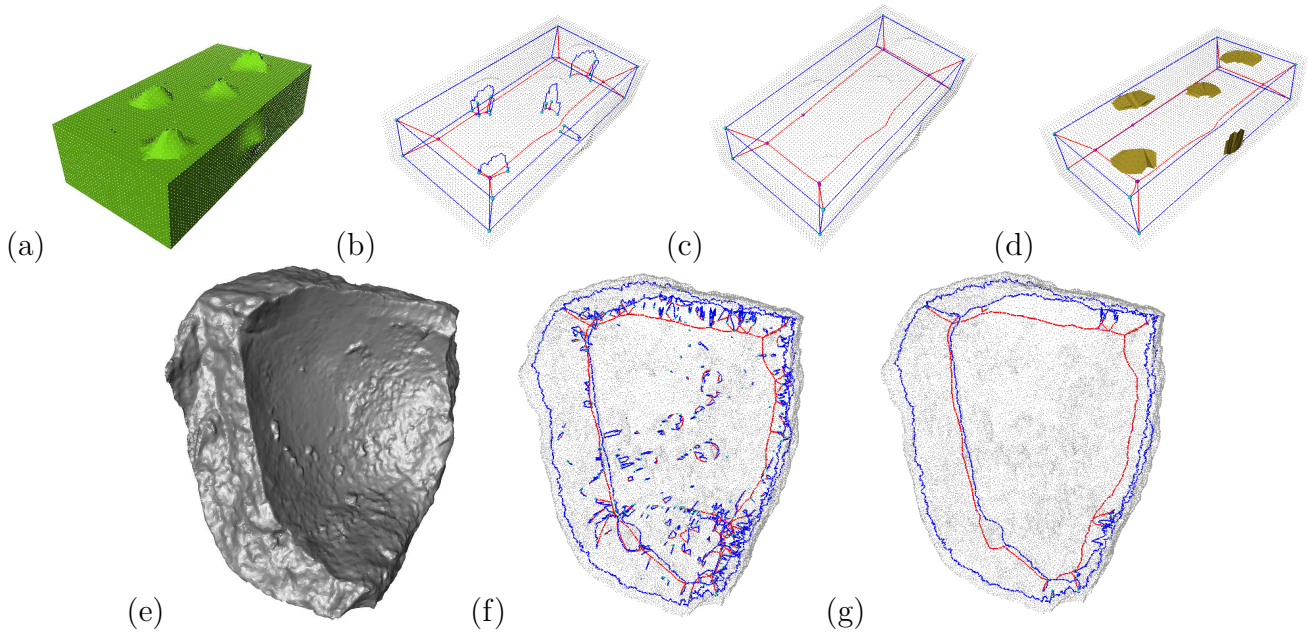

Figure 3: From [21], (a) Example of a rectangular box uniformly sampled, but perturbed by 5 protrusions (4 on top, 1 on a side). (b) Medial scaffold with the three types of transitions due to surface perturbations. (c) Regularized medial scaffold after transition removal. (d) The "cut off" patches (in yellow) corresponding to the removed transitions. (e) A pot sherd and (f) its medial scaffold. (g) medial scaffold after regularization.

axis in his analysis of the contraction of regions of 3-space onto their medial axis, and in particular in the codification of the 3D medial axis as a multi-tree structure [10, 9].

2 The Local Form of 3D Medial Axis for a generic surface

The goal of this paper is to study the transitions of the Medial Axis ($\mathcal{MA}$) of the smooth boundary S of a 3D shape as the shape evolves. The $\mathcal{MA}$ of S consists of the centers of 'maximal spheres' that is spheres which are tangent to S in more than one point and contained entirely inside the region bounded by S, together with limit points of this set (where the two or more contact points coincide).

The transitions are based on changes in the local form of the medial axis points of a smooth surface S in 3-space; there are five such local forms corresponding to the order of contact of the corresponding sphere of tangency (see for example [14]). We proceed to describe these types; see Figure 4.

$\mathbf{A_1^2}$: ordinary tangency between a sphere and S is referred to as A_1. The center of a sphere

tangent in this way at two distinct points—a 'bitangent sphere'—is an A_1^2 point of the $\mathcal{MA}$ and these are organized into sheets with other neighboring A_1^2 points. (See A in Figure 4.)

$\mathbf{A_1^3}$ or Y-junction point: this is the center of a sphere which is tangent at three distinct points of S. They organize into curves (A_1^3 curves or 'axes' or 'Y-junction curves') with neighboring A_1^3 points. For a tubular surface this represents a 'central axis'. Each A_1^3 curve is at the intersection of three A_1^2 sheets. (See B in Figure 4.)

$\mathbf{A_3}$ point: here, two contact points of a sphere with S come into coincidence; see the movement from (a) to (b) in the lower row of Figure 5. The sphere is then said to have contact A_3 with S (and to be a sphere of type A_3), while the center is an A_3 point of the $\mathcal{MA}$. These $\mathcal{MA}$ points form an A_3 curve, also called a *rim* or *rib* curve, which locally bounds a single A_1^2 sheet. The contact points of these spheres form a *ridge* or *crest line* on the surface. (For an extensive discussion of ridges, see [15].) (See C in Figure 4.)

$\mathbf{A_1^4}$ point: isolated spheres may have four ordinary (A_1) points of tangency with S. The center of such a sphere is an A_1^4 point of the $\mathcal{MA}$. These are generic, in contrast with five points of tangency or higher which disappear with small perturbations of the shape. The A_1^4 points lie at the intersection points of six A_1^2 sheets and four A_1^3 curves. For this reason, they are also called '6-junction points'. (See D in Figure 4.)

$\mathbf{A_1A_3}$ or fin point: the center of a sphere having ordinary (A_1) contact at one point and double (A_3) contact at another. These points are isolated from other A_1A_3 points, but, most significantly, both A_1^3 curves (Y-junction curves) and A_3 curves (rims or ribs) end at an A_1A_3 point. (See E in Figure 4.)

These five types of $\mathcal{MA}$ points, namely A_1^2 (sheets), A_1^3 and A_3 (curves), and, A_1^4 and A_1A_3 (points) are the only generic types of $\mathcal{MA}$ points in 3D. However, certain non-generic types such as A_1^5 (five ordinary tangency points) can occur when the surface changes shape in a generic way. A goal of this paper is to examine these cases.

In § 3 we examine how transitions, that is 'higher singularities' on the medial axis, can be understood by the 'collision' of medial axis points of the types described above, except for a few cases which are 'invisible' until the moment of transition. The possible collisions are limited by the geometry of the situation and also by some ideas from singularity theory. Thus we approach the problem from the opposite direction to Bogaevsky in [2, 3]: we ask how, from a geometrical viewpoint, the medial axis points can become more degenerate—

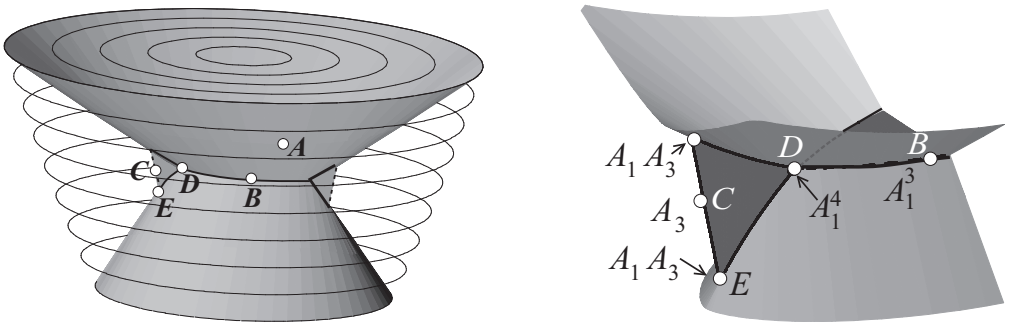

Figure 4: Left: A 'closed bin' with elliptical cross-sections, a top and a bottom, is indicated by contour lines only. The $\mathcal{MA}$ contains sheets of A_1^2 points (e.g. A: this is the center of a sphere tangent to front and top); curves of A_1^3 or Y-junction points (solid lines, e.g. B: tangency points top, bottom and front); curves of A_3 points (dashed lines, e.g. C: two tangency points coinciding at the left); isolated A_1^4 or 6-junction points (e.g. D: tangency points top, bottom, front and back); and isolated A_1A_3 or fin points (e.g. E: tangency points top and two coinciding at the right). Right: a close-up of the region around the A_1^4 point D showing the six sheets of the $\mathcal{MA}$ which meet there. One of these, a 'horizontal' sheet which consists of the centers of spheres which are tangent to the bin at the top and the bottom, is occluded in the left-hand figure. Note that four A_1^3 curves (dark lines) meet at D, one of them containing the point B.

more special—by means of 'events' such as collisions. The strict mathematical approach of Bogaevsky, which we describe briefly in § 4, starts from these degenerate situations and shows what they must look like *if* they arise in a generic family of surfaces. Finally, in § 5 we take the possible transitions one by one and construct an explicit example of each, which in addition is illustrated with computer drawn pictures, some for parametrized surfaces and some for point clouds extracted from images, and giving details of genericity requirements and other geometrical data to aid the understanding.

3 Description of the transitions of medial axes in 3D

3.1 Singularities

The distance function d from a point P in 3-space to a smooth surface S will have a minimum (indeed an absolute minimum) at X on the surface when P is the center of a sphere which is entirely inside the region enclosed by S and tangent to S at X: that is, X is the nearest point of S to P. The function d will have two equal (absolute) minima when P is the center of a bitangent sphere, tangent to S at two points X_1 and X_2 say. The value of d at X_1 and X_2 is equal to the radius of this sphere. Figure 5(a) illustrates this situation.

Singularity theory tells us which combinations of minima we can expect, both for a single

generic surface and in the situation where a surface evolves in shape in a generic way. In fact the meaning of the A_k notation (referred to as 'a singularity of d of type A_k') is that, in a suitable local system of coordinates (u, v) at X on the surface S, the distance function from the point P in 3-space takes the form $d(u, v) = u^2 + v^{k+1}$. Only odd values of k can make this a minimum; $k = 1$ is a nondegenerate minimum.

Now two minima can tend to coincidence, and this is what happens when two ordinary tangency points coincide at an A_3 point ($A_1^2 \to A_3$). Consider the family of functions parametrized by λ: $d_\lambda(u, v) = u^2 + v^4 - 2\lambda v^2$. For each $\lambda > 0$ this has an A_1 saddle at $(u, v) = (0, 0)$ and two A_1 minima at $(0, \pm\sqrt{\lambda})$. All three merge into one A_3 minimum for $\lambda = 0$ and for $\lambda < 0$ there is just one local minimum at $(u, v) = (0, 0)$. In an analogous way, as an A_1^2 point P on the $\mathcal{MA}$ approaches the A_3 curve, the two A_1 contact points between the sphere centered at P and the surface S merge (in Figure 4, a point just to the right of C having limit C). After the merger, there is only one local A_1 contact point, which does not contribute to the $\mathcal{MA}$. See Figure 5.

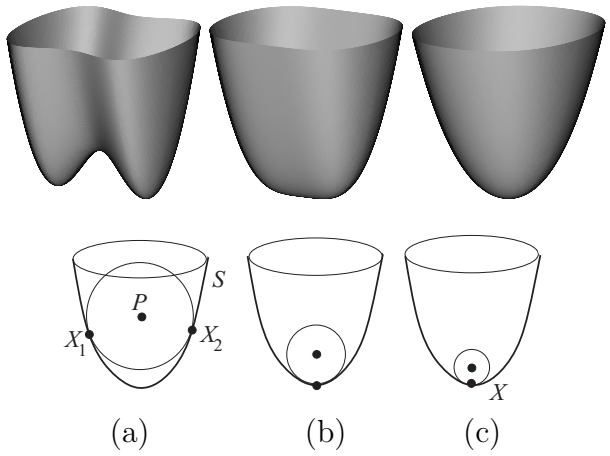

Figure 5: Top: graphs of the functions $d = u^2+v^4-2\lambda v^2$ for (a) $\lambda > 0$: two minima (A_1^2) at the same height and an A_1 saddle; (b) $\lambda = 0$: one degenerate (A_3) minimum; (c) $\lambda < 0$: one A_1 minimum. Bottom: (a) diagrammatic representation of a sphere tangent to a surface S in two points X_1, X_2, the distance function from the center P resembling the figure above, one minimum corresponding to each contact point. Similarly in (b) the two contact points have just coincided and the distance function has an A_3 minimum, and in (c) the sphere has ordinary A_1 contact just in one point X.

Similarly, moving along an A_1^3 curve we can encounter an A_1A_3 or fin point when two of the contact points merge: $A_1(A_1A_1) \to A_1(A_3)$. In Figure 4, this occurs as a point on the solid line south-west of E tends to E). We can also, of course, move directly on a path from A to E in Figure 4: $A_1^2 \to A_1A_3$.

Let us think of the four local coordinates on S of two points X_1 and X_2 and the three space coordinates of P as making up altogether 7 variables. To say that the sphere center P is tangent to S at X_1 and X_2 imposes 5 conditions: the distances from X_1 and X_2 to P are equal (1 condition) and the normals to S at X_1 and X_2 pass through P (2 conditions each). So we expect a $7-5=2$-dimensional solution, and indeed P moves on a 2-dimensional sheet of the $\mathcal{MA}$. The A_1^2 singularity is referred to as *codimension one* since P is confined to a set one dimension less than that of the ambient 3-space. For an introduction to these ideas of singularity theory see [5].

Singularity theory makes precise the notion of codimension for functions and also allows one to check that $A_1^3 = A_1A_1A_1$ and A_3 have codimension 2 (P is confined to curves) while A_1^4 and A_1A_3 have codimension 3 (P is confined to points). In general $A_kA_\ell\cdots$ has codimension $k+\ell+\cdots-1$. The theory predicts which kinds of singularities can merge together to form more degenerate ones. Also it predicts which additional singularities can occur when the surface is permitted to change shape in a generic way, governed by a new parameter t (time) say: this provides an extra variable so for example A_1^5 has codimension 4 and can now occur for isolated points P and moments of time t since together these give us four degrees of freedom.

There are certain geometrical situations where codimension can increase. For example, A_1^4—a sphere tangent in four places to S—usually has codimension 3, so occurs for isolated points of the $\mathcal{MA}$ of a generic surface, such as D of Figure 4. But if these four points are special, in fact if they are *coplanar*, then the codimension goes up to 4, and we expect to meet this only at isolated points and moments of time. This is the 'A_1^4 transition' which we will meet below; see Figure 15. There is one other case where this increase of codimension occurs, namely A_1A_3, which can also have codimension 4 in special configurations. These 'A_1A_3 transitions' are illustrated in Figures 17,18.

In principle we expect to meet all combinations of singularities whose codimension is ≤ 4, when studying distance functions on a family of surfaces evolving with one 'time' parameter t. (Only those giving minima are of interest for the $\mathcal{MA}$[1].) In addition, the ways in which singularities can merge (e.g. $A_1^3 \to A_1A_3$) is limited by general considerations from singularity theory: for a start, the codimension must *strictly increase*. See Figure 2.

However, in any special geometrical situation, such as that of distance functions, as opposed

[1]This rules out the so-called umbilic singularities, $D_4^{\pm}$, whose normal form is $u^3 \pm uv^2$ which is not a minimum.

to abstract families of functions, we have to check that all the 'expected' combinations actually occur. This is done, for example in [11] for the $\mathcal{MA}$ of a generic surface, and in the present article for families of surfaces. That is, the singularity theory limits what can possibly occur to a definite list, but it is then necessary to check explicitly which items in the list actually occur in the situation at hand. It is also desirable to explain their occurrence in a geometrical way, and our aim here is to do just that.

Codim-ension	Original singularity type	Singularities available close to it
4	A_5	A_1A_3, A_1^3, A_3, A_1^2
4	$A_1^2A_3$	A_1A_3, A_1^4, A_1^3, A_3, A_1^2
4	A_1^5	A_1^4, A_1^3, A_1^2
3*	A_1^4	A_1^3, A_1^2
3*	A_1A_3	A_1^3, A_3, A_1^2
2	A_1^3	A_1^2
2	A_3	A_1^2

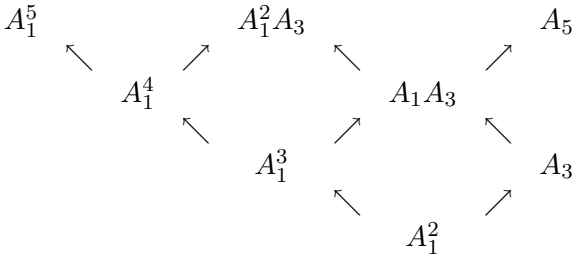

Figure 6: The table on the left lists the combinations of singularities which in principle can occur for distance functions on a surface evolving with one parameter (time t), and, in the third column, the singularity combinations which can exist in a neighbourhood. Thus in any row, the singularity combinations in the third column are available to merge into the singularity combination in the second column. (The two singularities with codimension marked with an asterisk * are those which have special configurations of codimension one higher; see the text.) The diagram on the right summarizes this information.

3.2 A geometrical view of the $\mathcal{MA}$ transitions

In this section, we shall systematically treat the various local transitions on the medial axis, using a number of geometrical principles to guide us, as well as the singularity-theoretic principles outlined in the preceding section. In §3.2.1 we consider those few cases in which a contact sphere can acquire an additional or more degenerate contact without effecting any change in the local topology of the medial axis; we call these 'invisible' since the change only occurs at the transitional moment itself. The remaining cases, in which singularities can be considered as visibly colliding on the medial axis, are covered in §3.2.2-3.2.5. All the visible cases are summarized in Tables 2 and 3.

3.2.1 'Invisible' transitions: Consider spheres with contact of the three types A_1^2 (on a sheet of the medial axis), A_1^3 (axis, Y-junction curve) and A_3 (rib line). In a perturbation of the surface it is possible for these three to acquire an additional point of contact in such a way that the connectivity of the medial axis is unaffected. This can only happen if the additional

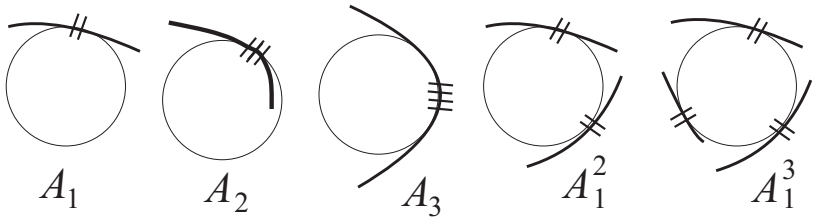

Figure 7: This figure illustrates the notation A_k^n in the context of the order of contacts with circles in 2D.

contact coincides (as a limit) with one of the existing contacts, turning an A_1 into an A_3 and an A_3 into an A_5; see Table 1.

Starting point	Event	Result	Figure
A_1^2	one A_1 becomes A_3	A_1A_3	17
A_1^3	one A_1 becomes A_3	$A_1^2A_3$	20
A_3	third contact coincides with A_3	A_5	23

Table 1: "Invisible" transitions.

No other possibilities yield generic singularities from the Table of Figure 2; it is noteworthy that the above three cases all correspond to 'double specializations' in the diagram of Figure 2. For a 1-parameter family of surfaces, the additional degree of freedom allows additional specializations beyond those expected for generic shapes; the latter make up the last three rows of the diagram. The transitions number seven two-step specializations in total, namely, $A_1^2 \to A_1^4$, $A_1^2 \to A_1A_3$, $A_1^3 \to A_1^5$, $A_1^3 \to A_1^2A_3$, $A_1^3 \to A_5$, $A_3 \to A_1^2A_3$, $A_3 \to A_5$. We can expect to observe all the two-step specializations, but the four not in Table 1, namely $A_1^2 \to A_1^4$, $A_1^3 \to A_1^5$, $A_1^3 \to A_5, A_3 \to A_1^2A_3$, require the addition of a contact point away from the pre-existing ones, which will change the connectivity of the medial axis. These are covered below.

3.2.2 Collisions of singularities: The five types of medial axis points can potentially give rise to 25 different 'collisions' where one singularity approaches another and they coalesce. A crucial ingredient of our enumeration of cases is the following proposition which states that singularities can only approach one another in a sheet of the medial axis.

Proposition 3.1 *Let P be a point of the medial axis of the surface S at which the singularity is of the simplest kind, A_1^2, so that the medial axis is* smooth *at P. We can therefore consider a sufficiently small neighborhood U of P in 3-space, contained inside the region D bounded by the maximal sphere whose center is P, and intersecting the medial axis in a smooth surface*

patch M. Then U does not contain any points of the medial axis of S besides those in M.

Proof. Let P^+ be one of the points of contact of the maximal (bitangent) sphere centered at P with S and let p be a point on the radius of this sphere from P to P^+ other than P itself. Suppose p is on the medial axis; then it is the center of a maximal sphere which bounds a solid ball D'. This ball D' cannot have the point P^+ in its interior since D' would then contain points outside S. In that case D' must be small enough to be entirely inside D, and of radius strictly smaller than the radius r of D. It follows that the points where the boundary sphere of D' is tangent to S must also be strictly inside D, which is impossible for a maximal sphere. It now follows that all the radii outwards from *smooth* points of the medial axis near P fail to contain points of the medial axis other than the points of the smooth A_1^2 sheet near P. But over a smooth piece of the medial axis the boundary retracts to the medial axis along the radii, so these radii fill out a neighborhood of P in the surrounding 3-space, and this completes the proof. □

The significance of this result is that in a transition, a branch of the medial axis does not approach a point of a smooth A_1^2 sheet *except along the smooth sheet itself.* It cannot approach through the 'empty space' between the sheets of the medial axis.

The key ingredient of the proof above is that the radial lines fill out a region of space. This also holds at A_1^3 and A_3 points, so we have:

Corollary 3.2 *The result of Proposition 3.1 holds also for the A_1^3 and A_3 cases, so that other points of the medial axis cannot approach these curves through the 'empty space' between the sheets, but only along the sheets or curves themselves.* □

Thus two A_1^3 curves cannot normally meet, but they can if they lie on the same sheet of the medial axis: they can then approach and become tangential. Again, A_3, A_1A_3 and A_1^4 points can only be 'approached' along sheets of the medial axis through them, not through the 'empty space' between the sheets.

When discussing the possible collisions of singularities, it will be useful to adopt a schematic approach. We shall consider two spheres, centered at points P and Q on a particular A_1^2 sheet Σ of the medial axis, namely (following Proposition 3.1) the sheet along which these singularities approach each other in the transition. These spheres are of types whose collision is being considered.

As an example, consider two different types A_1^4 and A_1A_3 (Figure 8). Suppose that they have contact with the boundary surface S at named points such as A, B, C, D for the A_1^4 and

$E = F, G$ for the A_1A_3, the symbol $E = F$ indicating that two contact points have coincided in an A_3. Each pair such as A, B corresponds to a sheet of the medial axis through P and we denote this sheet by AB: it consists of centers of spheres whose tangency points move away from A and B . Note that EF also legitimately denotes a sheet whose boundary, which we denote by rib(EF), is the A_3 curve (rib line) through Q. Let the family of surfaces S_t be parametrized by a 'time parameter' t, starting at $t = 0$, with $t = 1$ corresponding to the collision of the singularities. The two contact spheres will move continuously towards each other as t changes, making P, Q and the contact points functions of t. In the limit as $t \to 1$ the contact points on the first sphere must come into coincidence with those on the second sphere. There will be a number of ways in which this can happen, and we shall list these ways when considering a particular case. Suppose in the example that the sheet in which P and Q lie is $AB = EF$. Thus, for each point in time t, there is a path from P to Q in this sheet, and corresponding 'contact curves' on each S_t which are the traces of $A, B, E = F$ on S_t. Further, as $t \to 1$ and the path PQ shrinks to a point, these contact curves shrink to points, identifying A and B with the common limit of E and F.

The triple A, B, C defines an A_1^3 curve which we will label ABC; it lies in the medial sheet AB, as does the A_1^3 curve EFG; if one of the points C, D coincides with G at $t = 1$ then we can relabel if necessary so that it is C which does this. The sheet AB then contains two A_1^3 curves.

Proposition 3.3 *Whenever two A_1^3 curves lie in the same sheet AB, each having an endpoint, P and Q, respectively, and if P collides with Q, then either* (1) *at $t = 1$ the A_1^3 curves become aligned, that is have the same tangent, and merge into a single A_1^3 curve; or* (2) *the A_1^3 curves are in fact the same one, that is the points P and Q are connected by an A_1^3 curve in the sheet AB, and this A_1^3 curve shrinks to a point.*

To see this, note that the tangent line to an A_1^3 curve is determined by the positions of the three contact points on the sphere: the rule is that for distinct contact points the tangent to the A_1^3 curve is perpendicular to the plane of those points; and for points of the form $E = F, G$, it is perpendicular to the plane spanned by G and the principal direction at the ridge point $E = F$ corresponding to the ridge. See [14]. The result follows from this and the fact that these two triples of points on the two spheres have become identical at $t = 1$. (Note that the A_1^3 curves cannot become tangent pointing in the same direction (making a cusp) since the two spheres are both maximal.) $\square$

Note that, in contrast, A_3 curves, which are boundary rib-lines of sheets of the medial axis, cannot align as in (2) of the above proposition. If our points P and Q are endpoints of A_3 curves then, as $t \to 1$, the A_3 curve will shrink to a point.

3.2.3 Collision of points with points: Since there are two kinds of generic point singularities for a surface S, namely A_1^4 and A_1A_3, there are three cases to consider.

(a) Collisions of A_1^4 with A_1A_3 (Figure 8) As in the above discussion we can label the contact points for A_1^4 (center of sphere P) by A, B, C, D and those for A_1A_3 (center of sphere Q) by $E = F, G$. Then we can first use genericity to limit the possibilities as follows:

- Three of A, B, C, D cannot have the same limiting position as $t \to 1$ since this would produce a singularity A_5A_1 at least, hence not generic;
- If only one of A, B, C, D had the same limit as $E = F$ then we would have $A_1^3A_3$ at least, hence not generic;
- Hence, at least two, and hence exactly two of A, B, C, D have limit $E = F$ as $t \to 1$.
- Of the remaining two from A, B, C, D, one must have limit G and the other remain free, since other possibilities lead to non-generic singularities A_3^2 or $A_1^3A_3$. Hence *the limiting singularity must be* $A_1^2A_3$.

There is a further observation which, though not crucial, does help to reduce to two possible outcomes. Through Q, as through any A_1A_3 point, there is one A_1^3 curve and one A_3 curve. Through P, as through any A_1^4 point, there are four A_1^3 curves. On the other hand an $A_1^2A_3$ singularity will have *at most* four A_1^3 curves. (If the contact points of the A_1s are at X, Y say and the A_3 at Z then there are A_1^3 curves corresponding to contacts near (X, Y), (X, Z), (Y, Z) and (Z, Z).) Hence one A_1^3 curve certainly disappears in the transition, and there must therefore be such a curve joining P and Q. (Since this counts for both P and Q, in fact two A_1^3 curves will disappear.) There are three sheets through this (as through any) A_1^3 curve, so let us choose the sheet which also contains the A_3 curve at Q. Finally, let this sheet correspond with contact points A, B for the sphere centered at P. The sheet will contain A_1^3 curves ABC, ABD as well as the A_3 curve EF. The situation is illustrated schematically in Figure 8. Note that since the sheet AB is also the sheet EF, we have, as in Proposition 3.3, that the A_1^3 curves ACD, BCD, which are outside this sheet, must line up to have a common tangent as the singularities collide.

There are two possibilities: the curves ABD and rib(EF) can collide at another A_1A_3 before $t = 1$, or they can stay separate, depending on the angles in the figure. These lead

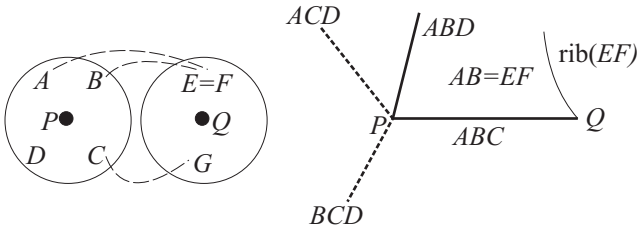

Figure 8: (§3.2.3(a)) A schematic representation of an A_1^4 at P and A_1A_3 at Q, before collision. The contact points are A, B, C, D for the first sphere and $E = F, G$ for the second. The A_1^3 curves are indicated by thick lines in the right-hand figure, those which are dashed being outside the sheet represented by the plane of the figure. The thin curve is the A_3 curve, rib(EF) which forms the boundary of the EF sheet. The thin dashed lines on the left indicate contact points which come together at the transition $t = 1$. The curves ABC and rib(EF) might collide in a further A_1A_3 or they might remain separate, giving two cases **(a1)** and **(a2)** as in the text.

respectively to **(a1)** $A_1^2A_3$-I $\uparrow$ (that is, in the upward direction of Figure 13); and to **(a2)** $A_1^2A_3$-II $\uparrow$. These are further illustrated in Figures 20 (right to center), 21 (right to center); see also Figure 19.

(b) Collisions of A_1^4 with A_1^4 (Figure 9) Let the contact points be A, B, C, D on the sphere center P and E, F, G, H on the sphere center Q, as in the schematic Figure 9. Using genericity, it follows that all of the points A, B, C, D must have different limits as $t \to 1$. For example, if A and B had the same limit then the result would be $A_1^3A_3$ at least. So there are two cases:
(b1) A, B, C, D have limits at the same points as E, F, G, H (we can assume they are in that order). Since the result is an A_1^4 singularity, *four* A_1^3 curves must disappear in the transition, that is, P and Q must be connected by two such curves. Choose one of the three sheets through one of these curves; without loss of generality we may assume this sheet is AB and EF, so that A and E become identified as $t \to 1$ and likewise B and F. We can then assume that the A_1^3 curve joining P and Q is ABC, and that the pairs (C, G) and (D, H) become identified. We therefore build up the diagram of Figure 9(a). In order for two A_1^3 curves to connect P and Q, two of the remaining A_1^3 curves must be identical and without loss of generality we can take these as ABD and EFH. Finally, we note that, using Proposition 3.3, the remaining A_1^3 curves, ACD and EGH must become tangent, and BCD, FGH likewise. But ACD, BCD become part of the same A_1^3 curve in the limit, so they must become tangent too and likewise EGH and FGH. So all four are tangent, which has the further consequence that the four contact points A, B, C, D (or E, F, G, H) are coplanar at $t = 1$. This corresponds to $A_1^4 \uparrow$ in Figure 13, and is further illustrated in Figures 15, 16, right to center.
(b2) Three of A, B, C have the same limits as E, F, G (say), and D and F remain free. This

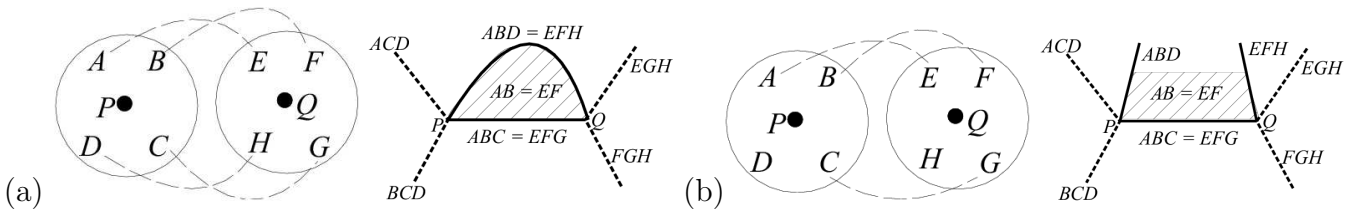

Figure 9: (§3.2.3(b)) A schematic representation of A_1^4s at P and Q, before collision. The contact points are A, B, C, D for the first sphere and E, F, G, H for the second. The thick lines are A_1^3 curves, dashed if they are not in the sheet represented by the plane of the diagram. Thin dashed lines are contact points which coincide at $t = 1$. (a) Represents the Case **3.2.3(b1)** in the text, resulting in an A_1^4 singularity where all the contact points are coplanar. (b) Represents Case **3.2.3(b2)**, where the result is A_1^5, but, depending on the angles, the A_1^3 curves ABD, EFH might or might not meet.

results in A_1^5. In this case, two A_1^3 curves must disappear in the transition, to leave the six expected at an A_1^5, so that P and Q are connected by such a curve in a sheet containing both of them. Since this curve shrinks to a point, the A_1^3s in question must be ABC and EFG and we can assume that the sheet is $AB = EF$. The figure is therefore the same as Figure 9(b) but now the two curves ABD, EFH will not be the same curve. Instead, there are two cases according as these curves collide, creating an A_1^4, or not. These are the two cases of $A_1^5 \uparrow$ and $A_1^5 \downarrow$, respectively in Figure 13, also illustrated in Figure 14.

(c) Collisions of A_1A_3 with A_1A_3 (Figures 10, 11) In this case there are a number of possible outcomes of the process of identifying the three contact points $A = B, C$ for the sphere centered at P with the three contact points $D = E, F$ for the sphere centered at Q, as $t \to 1$.

(c1) $A = B, C$ can all have limits at the same point, resulting in A_5; the only generic case then is for $D = E, F$ to have the same limit.

(c2) The points $A = B$ could identify with $D = E$, leaving C and F free; this results in $A_1^2A_3$.

(c3) The points $A = B$ could identify with $D = E$ and the points C and F could identify, resulting in A_1A_3 in the limit.

Case (c1) (Figure 10) In the case of A_5 there is *no* A_1^3 curve in the limit (this will be further studied in § 5; compare Remark 5.1). Hence the A_1^3 curves from P and Q must disappear, that is, P and Q are joined by such a curve, which as usual lies in three sheets of the medial axis, two of which are AB, with A_3 curve rib(AB), and DE, with A_3 curve rib(DE). The remaining sheet of those surrounding the A_1^3 curve can be labelled AC, BC, DF or EF. The situation is as in Figure 10(a). This is $A_5 \uparrow$ in Figure 13, which is also illustrated in Figure 23,

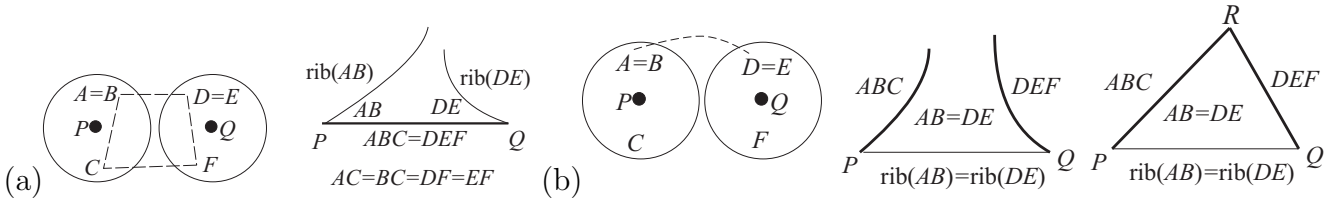

Figure 10: A_1A_3 collision with A_1A_3. (a) This represents Case **3.2.3(c1)** in the text, which results in an A_5 singularity. A schematic representation of A_1A_3s at P and Q, before collision, is shown (b). This represents Case **3.2.3(c2)** in the text, which results in an $A_1^2A_3$-II singularity. The A_1^3 curves ABC and DEF intersect at a further A_1^4 point R.

right to center.

Case (c2) (Figure 10) In this case, the A_3 contact curves AB and DE must connect since these are the only ones which shrink to a point as $t \to 1$. Thus we can use the common sheet $AB = DE$ for our diagram. This sheet will also contain the A_1^3 curves ABC and DEF, as in Figure 10(b). There is an interesting phenomenon at work here: by a general result on A_1A_3 points [14, §4.5], the tangents to the A_3 and A_1^3 curves at an A_1A_3 point are always coplanar with the normal to the surface and on the same side of it. Since the normals to the surface at contact points $A = B$ and $E = F$ coincide in the limit as $t \to 1$, the A_1^3 curves ABC and DEF are in fact forced to intersect, giving a further A_1^4 point R say as in Figure 10(b) right. Furthermore, as in Proposition 3.3, as the triangle formed shrinks to a point, the A_1^3 curves at R will align to become a single A_1^3 curve at $t = 1$. This is the situation of $A_1^2A_3$-II $\uparrow$ in Figure 13, which is also illustrated in Figure 21, right to center.

Case (c3) (Figure 11) The two A_1A_3 singularities at P and Q approach along a common sheet which could be $AB = DE$ or $AC = DF$. In either case this sheet contains the A_1^3 curve $ABC = DEF$. Hence, as in Proposition 3.3, P and Q either approach along an A_1^3 curve or are end-points of A_1^3 curves which align themselves as $t \to 1$. We draw the diagram using the sheet AB which because of the identifications of this case, will equal the sheet DE. There are essentially two cases, depicted in Figure 11. In the first case (left diagram), the two rib lines rib(AB) and rib(DE) must join since the curve PQ shrinks to a point. This is A_1A_3-I$\uparrow$ in Figure 13, also illustrated in Figure 17, right to left in (a). The second case (right diagram of Figure 11) is A_1A_3-II$\uparrow$ in Figure 13, also illustrated in Figure 18, right to center.

3.2.4 Collision of curves with curves: There are two kinds of curves, namely A_1^3 and A_3 curves. The fact that a collision must take place in a sheet of the medial axis containing both curves (Proposition 3.1 and Corollary 3.2) shows that, at the transition moment (called $t = 1$

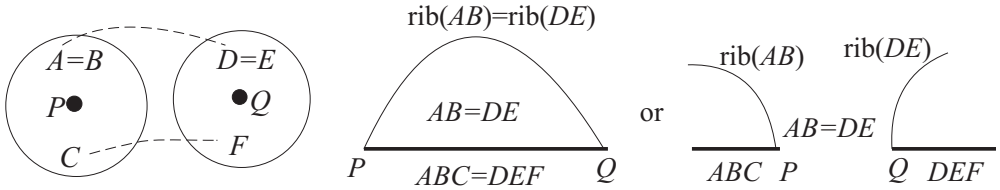

Figure 11: A_1A_3 collision with A_1A_3. This represents Case **3.2.3(c3)** in the text, which results in an A_1A_3-I (left) and A_1A_3-II (right) singularity.

in the discussion above), the curves must be tangential.

(a) In particular, when two A_1^3 curves collide, there will be a loss of two contact points, resulting in an A_1^4. In the notation used above, we have contact points A, B, C and D, E, F say, and collision takes place in (say) the sheet $AB = DE$, the two A_1^3 curves being ABC and DEF. Then at the transition, the points A and D coincide, and B and E coincide, leaving C and F free and making four contact points. Furthermore, since the tangents to ABC and DEF are the same at the collision point, the triangles ABC and DEF have the same normal[2], so that the four contact points are *coplanar*. This is the transition $A_1^4 \downarrow$ in Figure 13; compare Case (b1) in §3.2.3. See also Figures 15 and 16, left to center.

(b) When an A_1^3 and an A_3 curve collide. moving in a sheet of the medial axis, the curves become tangential at the transition moment. With contact points A, B, C and $D = E, F$, the sheet is DE, and this must equal one of the sheets obtained from A, B, C, say AB. So A and B both have the same limit as $D = E$, and since the A_1^3 curve ABC and the A_3 curve rib(DE) become tangential, we must have C, F having the same limit. The result is therefore an A_1A_3 singularity, as in A_1A_3- II$\downarrow$ of Figure 13. See also Figure 18, left to center.

The collision of two A_3 curves in one sheet is not generically possible since the points of contact of the corresponding maximal spheres must be on opposite sides of the sheet and therefore the result will be a non-generic A_3^2 singularity. It is worth remarking here that generic evolution of A_3 curves (ridges crest lines) in a 1-parameter family of surfaces has been examined in detail in [6]. Two ridges can indeed collide, but this event always involves A_4 points ('turning points'), that is spheres where the contact is of a type which cannot occur for the medial axis since it does not represent a minimum of the distance function (compare § 3.1). Thus as far as the medial axis is concerned, the events are not visible. The A_5 transition, described in Case (c1) of §3.2.3 and in §5, also involves A_4 points but here two of them come together and disappear in the transition, making it visible on the medial axis.

[2]The rule for determining the tangent to an A_1^3 curve is recalled in the proof of Proposition 3.3 above.

3.2.5 Collisions of curves with points: There are four cases to consider. Cases (a) and (b) below are illustrated in Figure 12.

(a) A_1^3 and A_1^4 Let the contact points be A, B, C and D, E, F, G and let the common sheet be $AB = DE$; see Figure 12(a) for a schematic picture. However, the angle between any two A_1^3 branches at an A_1^4 is less than 180° in the sheet in which they lie[3]. So what actually happens is that the two A_1^3 branches DEF, DEG meet the branch ABC before the transition, making generic A_1^4 singularities via an A_1^4 transition; the result is a 'triangle' of A_1^4s which disappears in the transition, as in $A_1^5 \uparrow$ of Figure 13, also Figure 14, right to center.

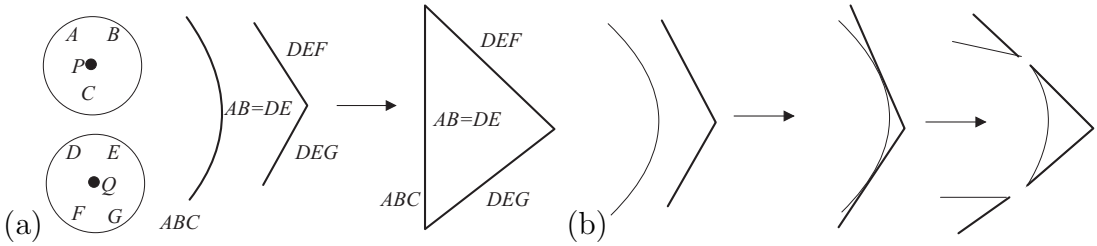

Figure 12: See §3.2.5. (a) The collision of an A_1^3 curve and an A_1^4 point actually produces a 'triangle' of A_1^4 points which collapses during the transition to an A_1^5. (b) The collision of an A_3 curve and an A_1^4 point actually produces a 'triangle' of two A_1A_3 points and an A_1^4 point which collapses during the transition to an $A_1^2A_3$. Thick lines are A_1^3 curves and thin ones are A_3 curves.

(b) A_3 and A_1^4 This is a analogous to the case just considered. Working in the sheet containing the A_3 curve, the angle property of A_1^4 points ensures that, before the transition, there will be tangency between the A_3 curve and two A_1^3 branches in the same sheet, as in (a) above. The result is a 'triangle', two of whose vertices are A_1A_3 points and the other one an A_1^4 point, which collapses in the transition, Figure 12(b). This corresponds with $A_1^2A_3$-II$\uparrow$ of Figure 13 and has in fact been met above, as Case (a2) of §3.2.3, see also Figure 21, right to center.

(c) A_1^3 and A_1A_3 This one is straightforward to analyse by the same means; the result is $A_1^2A_3$-I$\downarrow$ in Figure 13. See also Figures 20, left to center and 19, center to right.

(d) A_3 and A_1A_3. Let the contact points be $A = B$ and $C = D, E$. To avoid a non-generic A_3^2 singularity, the common sheet must be $AB = CE$ (rather than $AB = CD$), and the A_1^3 curve CDE lies in this sheet. But this implies that all of $A = B, C = D, E$ have the same limit point at the collision, that is, the sphere has A_5 contact. But the A_5 singularity has no A_1^3 curve (compare Remark 5.1) so in fact the A_1^3 curve CDE must shrink to a point, hence there must be another A_1A_3 point which collapses at the same time. This is the $A_5 \uparrow$ transition of Figure 13, already encountered in Case (c1) of §3.2.3, Figure 23, right to center.

[3] For a detailed analysis of the A_1^4 configuration, see [14].

Reference	Collision of singularities	Transition (Fig. 13)	Figures illustrating transitions
§3.2.3(a1)	A_1^4 with A_1A_3	$A_1^2A_3$-I↑	Fig. 20 right to center; Fig. 19, right to center
§3.2.3(a2)	A_1^4 with A_1A_3	$A_1^2A_3$-II↑	Fig. 21 right to center; Fig. 19, center to left
§3.2.3(b1)	A_1^4 with A_1^4	A_1^4 ↑	Fig. 16 right to center; Fig. 15 right to center
§3.2.3(b2)	A_1^4 with A_1^4	A_1^5 ↑	Fig. 14 right to center
§3.2.3(b2)	A_1^4 with A_1^4	A_1^5 ↓	Fig. 14 left to center
§3.2.3(c1)	A_1A_3 with A_1A_3	A_5 ↑	Fig. 23 right to center
§3.2.3(c2)	A_1A_3 with A_1A_3	$A_1^2A_3$-II↑	Fig. 21 right to center; Fig. 19, center to left
§3.2.3(c3)	A_1A_3 with A_1A_3	A_1A_3-I↑	Fig. 17 right to left
§3.2.3(c3)	A_1A_3 with A_1A_3	A_1A_3-II↑	Fig. 18 right to center
§3.2.4(a)	A_1^3 with A_1^3	A_1^4 ↓	Fig. 15 left to center; Fig. 16 left to center
§3.2.4(b)	A_1^3 with A_3	A_1A_3-II↓	Fig. 18 left to center
	A_3 with A_3	not possible	——
§3.2.5(a)	A_1^3 with A_1^4	A_1^5 ↑	Fig. 14 right to center
§3.2.5(b)	A_3 with A_1^4	$A_1^2A_3$-II↑	Fig. 21 right to center; Fig. 19, center to left
§3.2.5(c)	A_1^3 with A_1A_3	$A_1^2A_3$-I↓	Fig. 20 left to center; Fig. 19, center to right
§3.2.5(d)	A_3 with A_1A_3	A_5 ↑	Fig. 23 right to center

Table 2: A summary of transitions arising from collision of point and curve singularities. §3.2.3 is point with point; §3.2.4 is curve with curve and §3.2.5 is point with curve.

4 Relationship with the work of Bogaevsky

In [2, 3], I.A. Bogaevsky examines several related problems connected with the classification of transitions (perestroikas) of 'minimum functions'. That is, we consider a local family of functions of the form $F(t, \mathbf{x}) = \min f(t, \mathbf{x}, \mathbf{y})$ where t is a 'time' parameter (so a single real parameter), $\mathbf{x} \in \mathbf{R}^3$ and $\mathbf{y}$, over which the minimum is taken, is in a Euclidean space which for the medial axis application would be 2-dimensional, corresponding to the 2-dimensional surface S whose medial axis is being considered. For each value of t close to some t_0 (the moment of transition) we can consider the set X of points $\mathbf{x}$ for which F is not differentiable. Bogaevsky provides a complete list of these transitions, provided the function f is generic.

There are also two special cases considered. The first one, described as 'shocks' (these are not the same as the shocks which we associate with a dynamical construction of the medial axis) is one to which an 'arrow of time' can be associated, where in fact the local topology of the set X as above is 'trivial' (homotopic to a point) for all $t \geq t_0$: we might say loosely that moving through the transition from $t < t_0$ to $t > t_0$ 'simplifies the topology.'

The second special case is the one which concerns us most closely. Here, the topology of X is trivial for all t close to t_0, and this corresponds to the well-known fact that the medial axis of a smooth compact connected surface is locally contractible to a point. The resulting transitions are shown in Figure 13, reproduced from Bogaevsky's work, in which he has used

Transitions in Figure 13	Collision of singularities	Figures
A_1A_3-I	$(A_1A_3,\ A_1A_3)$	17←
A_1A_3-II	$(A_1A_3,\ A_1A_3)$	18←
A_1A_3-II	$(A_1^3,\ A_3)$	18→
A_1^4	$(A_1^4,\ A_1^4)$	15←, 16←
A_1^4	$(A_1^3,\ A_1^3)$	15→, 16→
A_1^5	$(A_1^4,\ A_1^4)$	14←
A_1^5	$(A_1^4,\ A_1^4)$	14→
A_1^5	$(A_1^3,\ A_1^4)$	14←
A_5	$(A_1A_3,\ A_1A_3)$	23←
A_5	$(A_3,\ A_1A_3)$	23←
$A_1^2A_3$-I	$(A_1^4,\ A_1A_3)$	20←
$A_1^2A_3$-I	$(A_1^3,\ A_1A_3)$	20→
$A_1^2A_3$-II	$(A_1^4,\ A_1A_3)$	21←
$A_1^2A_3$-II	$(A_1A_3,\ A_1A_3)$	21←
$A_1^2A_3$-II	$(A_3,\ A_1^4)$	21←

Table 3: A summary of the generic ways transitions can arise from collision of point and curve singularities.

topological and some algebraic constraints to narrow down the list from a larger one. In principle these might still include some extras which cannot occur for surfaces (there might in principle be other constraints), but in §5 we in fact exhibit an explicit family of surfaces for which the medial axis undergoes each transition in turn. There is also the assumption that the family of distance functions is generic[4]. Thus in our situation we have a family of surfaces parametrized say by $\Gamma(t, \mathbf{y})$ where t is the 1-dimensional time parameter and $\mathbf{y}$ is 2-dimensional. We then define $f(t, \mathbf{x}, \mathbf{y}) = ||\mathbf{x} - \Gamma(t, \mathbf{y})||^2$. The usual medial axis is simply the set of points for which the corresponding minimum function (minimum over $\mathbf{y}$) is not differentiable.

5 Examples and Illustrations

In this section we shall present explicit examples of the transitions described in §3. This serves two purposes. One is to show that the theoretically derived transitions can actually occur—this does not follow from either our geometrical arguments or from the results of Bogaevsky in §4. Note that in order to show that the theoretical transitions *really* occur we need to verify

[4]A technical difficulty that has so far not been resolved is whether this is equivalent to studying the transitions of the medial axis for a generic 1-parameter family of generic surfaces. Previous examples where this problem has arisen (*e.g.,* the study of caustics by reflection) have been answered positively, but each case needs a separate and rather lengthy investigation.

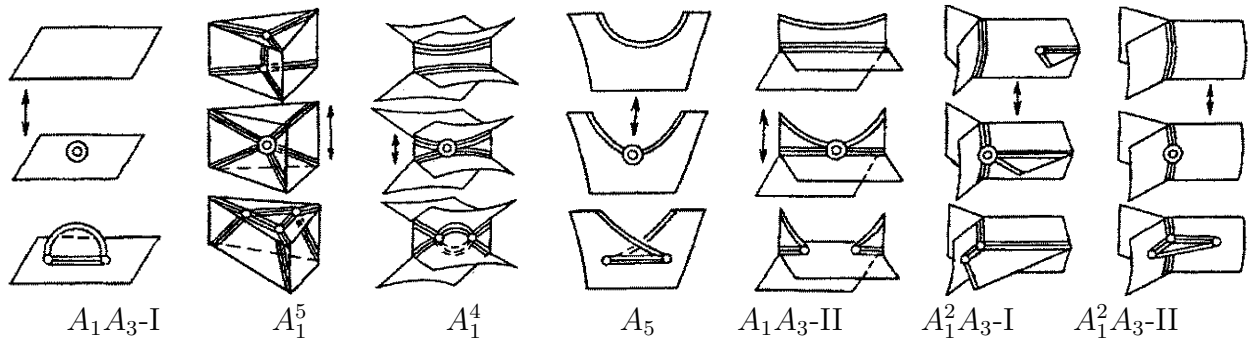

Figure 13: A summary figure of those singularities (perestroikas) that relate to the transitions of the medial axis in 3D, as presented by Bogaevsky in [2, 3]. Double lines represent A_3 curves, triple lines represent A_1^3 curves (Y-junction curves), small circles represent A_1A_3 (fin) points, and double circles represent higher singularities.

that our models satisfy certain technical genericity conditions. This is done in [24]; here we shall merely mention from time to time the result of checking these conditions. The second equally important purpose is to guide the intuition in understanding what is happening during the transitions by exhibiting a simple occurrence of each one.

1) The A_1^5 transition: This can be generated quite easily by taking five planes tangent to a sphere, for example making a triangular prism. One of the sides of the triangle can now be moved so that the sphere remains tangent to four planes but loses contact with the fifth. Depending on which way the side moves, either two or three A_1^4 points are created on the medial axis. This is illustrated in Figure 14, where the five planes are $x = 0,\ y = 0,\ z = 0,\ z = 1$ and $ax + 4y = 12$. The transition is obtained by allowing a to pass through the value 3. The first figure shows just the A_1^3 lines, drawn exactly, and the second shows a simulation by F. Leymarie, using the techniques of [20].

2) The A_1^4 Transition: There are a number of ways of generating this transition. One is by starting with a surface S whose horizontal sections are ellipses, say $2x^2 + y^2 = z + 1$, which we cut by planes $z = 0, z = k > 0$ forming a 'lid' and 'base' to the object. As k decreases, there will come a critical moment at which there exists a sphere tangent to both lid and base and tangent twice to the elliptical cylinder S, at 'front and back', and entirely contained within the closed object. Calculation shows this to occur at $k = \sqrt{2} + \frac{1}{2}$. These four contact points will automatically be coplanar, and the transition is observed as the ends continue to come closer together.

Figure 15, left, shows the curved surface of S (without the lid and base) and the medial axis for a value of k large enough that there is *no* sphere tangent to the lid and the base which

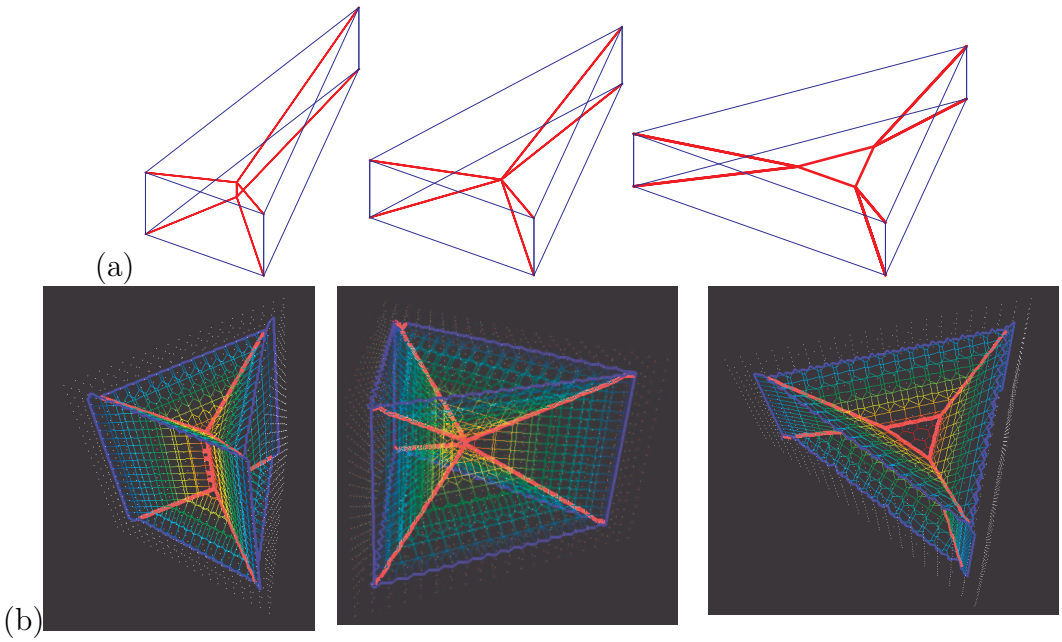

Figure 14: (a) An A_1^5 transition is illustrated through the change in the A_1^3 lines. This left to right direction here corresponds to the downwards direction of A_1^5 in Figure 13. In this model, the outer straight edges of the 'wedge of cheese' count as A_3 lines. (b) A different simulation of the same shape. Both directions have been described as a collision of A_1^4 points in §3.2.3(b2). The right-to-center transition has also been described as a collision of an A_1^3 curve and an A_1^4 point in §3.2.5(a).

fits inside. This figure was produced by means of exact calculation and a Maple program. The next three parts of this figure show, using the program of F. Leymarie, the A_3 and A_1^3 curves of the medial axis through the transition. When the lid and base are close enough, there is a horizontal A_1^2 sheet containing centers of spheres tangent to the lid and the base. An exact figure is in Figure 15, extreme right and also in Figure **??**. Another example, the squeezed tube, is shown in Figure 16.

Note on genericity In order to generate this transition we need the four contact points of the A_1^4 sphere to be coplanar. In a family of surfaces these contact points will move continuously. To generate a generic transition we need also this movement to have the effect that (i) the points become non-coplanar, (ii) each contact point moves in a direction that is not tangential to the sphere at that point. For more details, see [24].

3) The A_1A_3-I Transition : Consider a medial axis sheet (A_1^2 points) arising from two boundary surfaces. An analogous perturbation to the planar example in Figure 1 occurs when one of the boundary surfaces is protruded to form a bump. A good example of a generic bump is a two-dimensional Gaussian with asymmetric sigmas, that is,

$$z = f(x, y) = A \exp\left(\frac{-x^2}{2\sigma_x^2}\right) \exp\left(\frac{-y^2}{2\sigma_y^2}\right) \qquad \text{where } \sigma_x < \sigma_y. \tag{1}$$

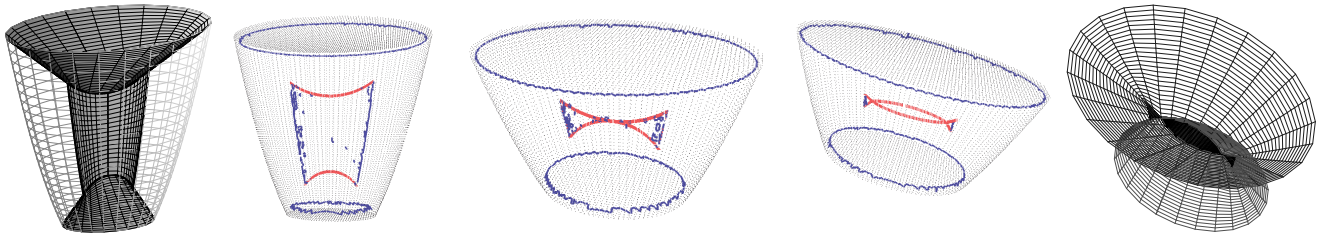

Figure 15: Illustration of the A_1^4 transition. Far left: an 'elliptical cylinder with flat ends' (the ends are not drawn) and its medial axis, plotted using MAPLE and exact calculation. The next three figures show the A_3 and A_1^3 curves evolving through the transition, as the ends of the cylinder become closer together. Left to right is the *downwards* transition in Figure 13. Two A_1^4 points are created in this transition, visible in the figure on the right as crossings of the A_1^3 curve; see also §3.2.4(a). Right to center has been described in §3.2.3(b1). Far right: an exact calculation of the medial axis after the creation of A_1^4 points, with three of the A_1^2 sheets drawn in black and the other two larger sheets in wireframe.

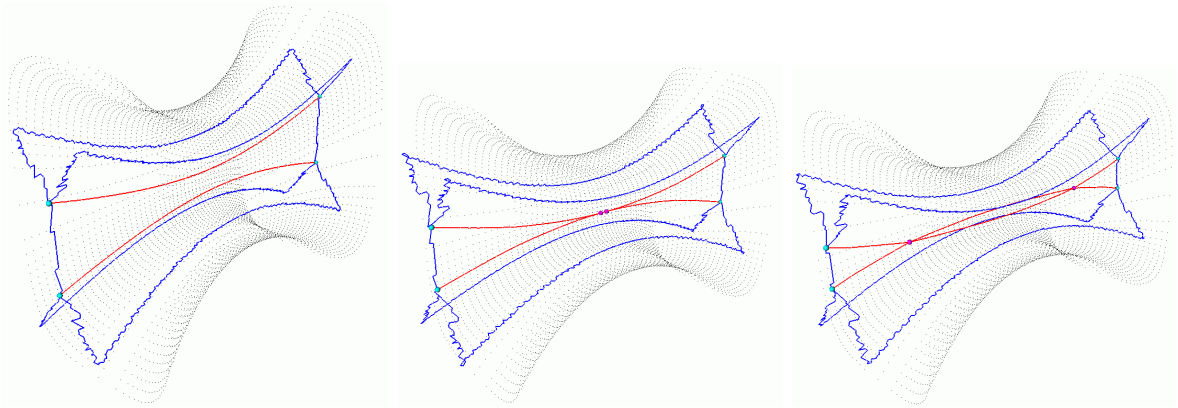

Figure 16: Another realization of an A_1^4 transition, obtained by 'squeezing' a tube. Left to right is the transition in the *downward* direction in Figure 13, and left to center has been described as a collision of two A_1^3 curves in §3.2.4(a). The transition right to center has been described as a collision of two A_1^4 points in §3.2.3(b1).

Since the larger principal curvature is along the yz plane, the medial axis sheet arises from the centers of curvature of the curve $z = f(x, 0)$, whose curvature $\kappa(x)$ given by

$$\kappa(x) = \frac{f''(x,0)}{(1+f'(x,0)^2)^{\frac{3}{2}}} = \frac{A}{\sigma_x^4} \exp\left(\frac{-x^2}{2\sigma_x^2}\right)\left(x^2 - \sigma_x^2\right).$$

In particular, $\kappa(0) = -A/\sigma_x^2$. This implies that in the absence of additional structure, the Gaussian bump will form an A_3 point at $\left(0, 0, f(0,0) + \frac{1}{\kappa(0)} = A - \frac{\sigma_x^2}{A}\right)$. For a bump which is barely visible, the ratio of σ_x^2 to A is very high, that is the spread of the protrusion is much larger than its magnitude. Thus, the center of curvature forms very far from the peak and the presence of any other structure typically prevents the formation of the A_3 point. As the salience of the bump increases in a one parameter family of perturbations, *i.e.*, as the ratio $\frac{\sigma_x^2}{A}$ decreases, at some point the (thus far non-maximal) sphere of curvature of the bump also forms a contact elsewhere, forming an A_1A_3 transition. This is parallel to the 2D case shown

in Figure 1(a). From this point onward, the sphere is maximal and the corresponding medial point emerges, undisturbed by other structure. Figure 17 shows a simulation with $\sigma_y = 2.5$, $\sigma_x = 1$.

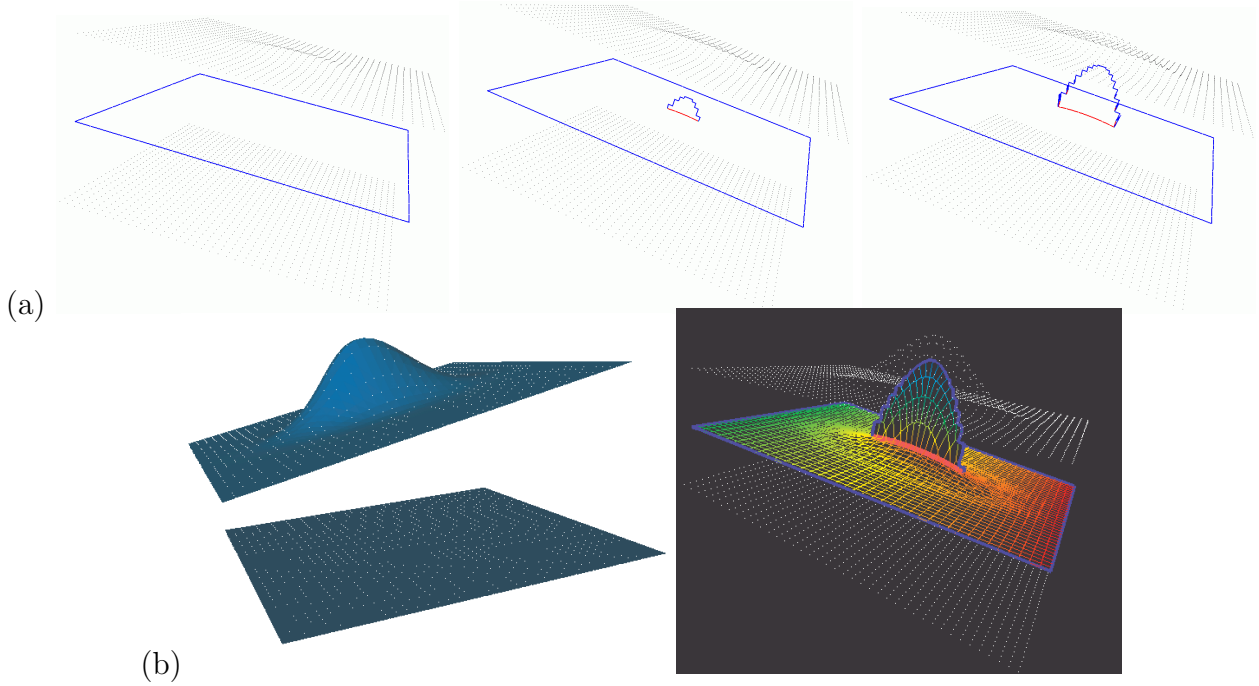

(a)

(b)

Figure 17: The A_1A_3-I transition during which a 'fin' passes through another sheet of the medial axis, caused by a rising bulge in the upper boundary surface. The moment of appearance of the fin is described as an invisible transition in §3.2.1, and the reverse transition, where the fin disappears, as a collision of two A_1A_3 points in §3.2.3(c3). (b) A different view of the figure on the right in (a).

4) The A_1A_3-II transition: In this transition two curves, one A_3 and one A_1^3, approach each other, become tangent, and then split into two portions each, grouped at two new A_1A_3 points. It is rather straightforward to generate examples for this transition: by 'flattening' a ridge, its A_3 (rim or rib) curve on the medial axis moves away from the ridge and into the A_1^2 sheet it is on. If this sheet is bounded by an A_1^3 curve elsewhere, the A_3 and A_1^3 curves can eventually collide. Alternatively, the ridge can be fixed and the 'width' of the shape can be reduced, thus moving the A_1^3 curve closer to the A_3 curve, with the same effect. In the first case, we sweep a parabola along the z axis, widening it at $z = 0$, and closing it up with a 'top' at $y = 1$. Note that the parabola $y = ax^2$ has curvature $2a$ at its vertex, so that when swept it generates a ridge and a corresponding A_3 curve (rib). By a modification, we can make this parabola bulge in the middle while keeping $z = \pm 1$ sections constant, for example by $y = [a_1(1 - z^2) + a_2 z^2]\, x^2$, so that at $z = 0$ the curvature of the cross section is $2a_1$, while at $z = \pm 1$ the curvature of the section is $2a_2$. This is illustrated in Figure 18.

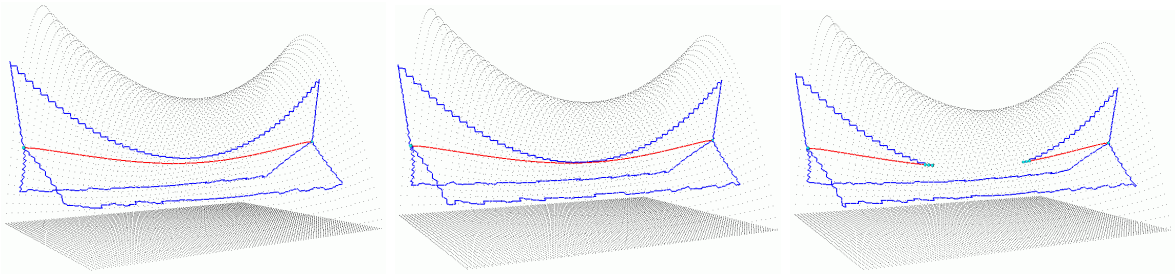

Figure 18: Computation of an A_1A_3-II transition. This can be regarded, left to center, as the collision of an A_1^3 curve with an A_3 curve, as in §3.2.4(b), and, right to center, as the collision of two A_1A_3 points, as in §3.2.3(c3). The *down* direction in Figure 13 is left to right in this figure.

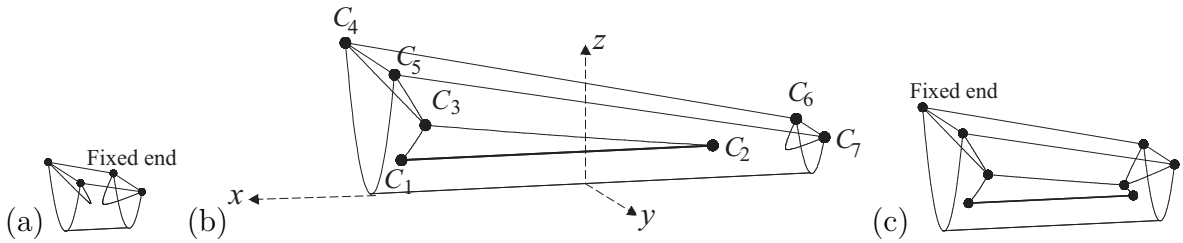

Figure 19: The 'parabolic gutter with two ends and a roof' used in the text to describe the two $A_1^2A_3$ transitions. The figures show the 1-dimensional strata of the medial axis: the A_1^3 curves which are drawn thinly, and the A_3 curve C_1C_2 in (b) and a similar curve in (c) which are drawn thickly. Note that all the sharp corners of the gutter—along four straight edges defining the 'roof' $C_4C_5C_7C_6$ and along two parabolic edges at the ends—also count as A_3 curves in this model. The points C_1, C_2 (and also C_4, C_5, C_6 and C_7) are A_1A_3 points, while C_3 and the similar point in (c) are A_1^4 points. For $A_1^2A_3$-II take (a) and (b) and ignore the right-hand ends which remain fixed in the deformation process. From (a) to (b) is the transition *downwards* in Figure 13. For $A_1^2A_3$-I take (b) and (c) and ignore the left-hand ends which remain fixed in the deformation process. From (b) to (c) is the transition *downwards* in Figure 13.

5,6) The $A_1^2A_3$ Transitions

Both of these can be illustrated in the same way. In fact consider a surface (Figure 19(b)) made up of four sheets (i) a parabolic 'gutter': a sheet $z = ay^2$, of constant curvature along the ridge which coincides with the x-axis; (ii) an end plane $x = p$ for some $p > 0$ say; (iii) an end plane $x = q$ for some $q < 0$; (iv) a sloping 'roof' given by a plane $z = bx + c$ where b and c are > 0. We shall want to avoid the sloping roof cutting the x, y plane so we need to have $bq + c > 0$. We can arrange for the $A_1^2A_3$-II transition to occur by keeping q fixed and moving p from large to small positive values, and for the $A_1^2A_3$-I transition to occur by keeping p fixed and moving q from large to small negative values. We now proceed to explain the details.

$A_1^2A_3$-I Case For this case we ignore the $x = p$ end (the left-hand end in Figure 19(b)). The A_1A_3 point C_2 (the coordinates are given in (5) below) remains in place. There is an A_1^3 curve connecting the corners C_6, C_7 at the top of the $x = q$ end where this end meets the

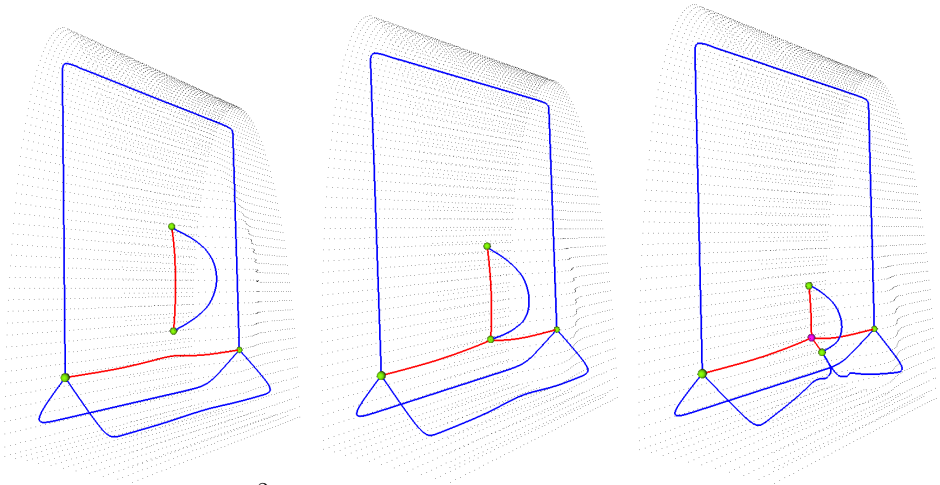

Figure 20: Computation of an $A_1^2A_3$-I transition. The *down* direction in Figure 13 is left to right in this figure. Left to center has been described as a collision between an A_1A_3 point and an A_1^3 curve in §3.2.5(c), and right to center as a collision between A_1^4 and A_1A_3 points in §3.2.3(a1).

roof. This A_1^3 curve consists of centers of spheres tangent once to the gutter and tangent to the roof and to the $x = q$ end. It crosses the plane of symmetry $y = 0$ at $(q + \lambda, 0, \lambda)$, where $\lambda = (c + bq)/(1 - b + \sqrt{1 + b^2})$. This point is on the medial axis provided the radius of the sphere (which is the z-coordinate λ of the center) is $\leq 1/2a$. This requires

$$q \leq \frac{1 - b + \sqrt{1 + b^2} - 2ac}{2ab}. \tag{2}$$

In this case the A_1^3 curve passes uninterrupted from C_6 to C_7; when $y = 0$ on this A_1^3 curve the sphere is tangent to the ridge curve on the gutter and is smaller than the sphere of curvature there, so contributes to the medial axis. If λ takes the value $1/2a$, making equality in (2) then the point C_6 is an $A_1^2A_3$ point, the sphere having A_3 tangency to the gutter and A_1 tangency to the roof and to the end $x = q$. Furthermore substituting for λ we find that the A_3 line (the rib) has reached the A_1^3 curve from C_6 to C_7 and pierced it to produce an $A_1^2A_3$-I transition. For values of q making $\geq$ in (2) there will be an A_1^4 point as in Figure 19(c): a sphere is tangent twice to the gutter and tangent to the roof and the $x = q$ end. See also Figure 20 for a different example of this transition.

$A_1^2A_3$-II Case For this let us ignore the $x = q$ end—the right-hand end in Figure 19. There is an A_3 (rib) curve consisting of points of the form $(t, 0, \frac{1}{2a})$, but only part of this will lie on the medial axis: the sphere centered at this point and of radius $1/2a$ must avoid bumping into the ends and the roof. Since the sphere has constant radius and the roof slopes down from the 'left' $x = p$ end to the 'right' $x = q$ end, we need only prevent the sphere from bumping into the $x = p$ end and into the roof. This requires

$$\frac{1 + \sqrt{1 + b^2} - 2ac}{2ab} \leq t \leq p - \frac{1}{2a}. \tag{3}$$

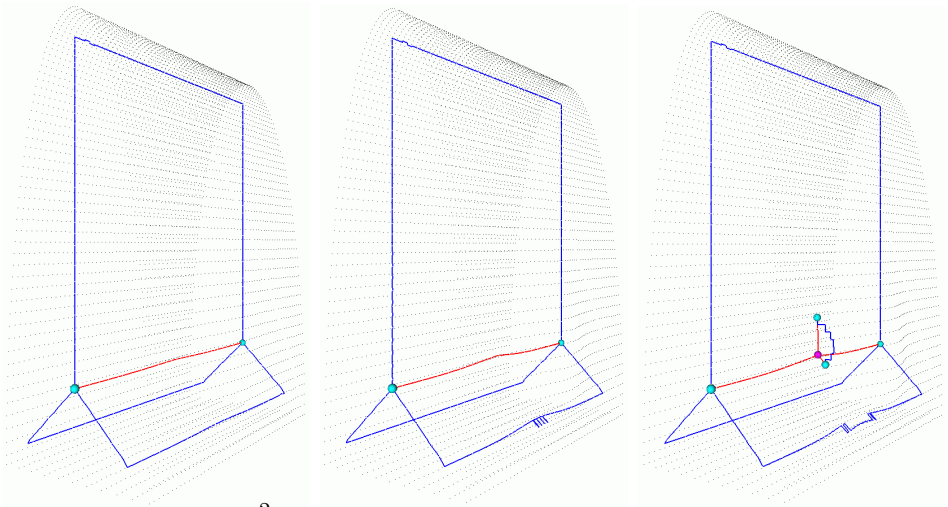

Figure 21: Computation of an $A_1^2A_3$-II transition. The *down* direction in Figure 13 is left to right in this figure. Right to center is also described as a collision of points in §3.2.3(a2,c2), and as a collision of an A_3 curve and an A_1^4 point in §3.2.5(b). Left to center is an 'invisible' transition as in §3.2.1.

For solutions we require that

$$p \geq \frac{1+b+\sqrt{1+b^2}-2ac}{2ab}. \tag{4}$$

If there is $<$ in (4) then there is no A_3 curve on the medial axis, as in Figure 19(a). If there is $=$ then at this transitional moment a unique t exists, the corresponding center being an $A_1^2A_3$ point; and with $>$ there is a finite length of A_3 curve, as in Figure 19(b). By allowing p to pass through the value giving $=$ in (4) the $A_1^2A_3$-II transition is realised. With $>$ in (4) the two ends of the A_1^3 curve are A_1A_3 points, given by taking t to have the extreme values in (3), say C_1 is the medial axis point given by the higher extreme value and C_2 that given by the lower:

$$C_1 = \left(p - \frac{1}{2a}, 0, ay^2\right), \quad C_2 = \left(\frac{1+\sqrt{1+b^2}-2ac}{2ab}, 0, \frac{1}{2a}\right). \tag{5}$$

From each of these an A_1^3 curve will emanate: from C_1 this corresponds to spheres having contact in three points: twice with the parabolic gutter and maintaining contact with the end $x = p$; from C_2 the A_1^3 curve corresponds to spheres having contact twice with the parabolic gutter and maintaining contact with the sloping roof. These A_1^3 curves will end in the center C_3 of the sphere having contact twice with the gutter and with both flat end and roof. With $<$ in (4) there is no A_3 curve and these A_1^3 curves have disappeared too. What is left is an A_1^3 curve joining the top corners, C_4 and C_5 say, of the end $x = p$, where this meets the roof, as in Figure 19(a). A different example is given in Figure 21.

Notes on genericity The geometrical conditions for the $A_1^2A_3$ singularities to occur, and to be generic transitions, can be expressed in terms of the osculating plane Ω of the line of curvature at the ridge (A_3) point. They have been determined in [24] and are as follows.

(The above examples satisfy these conditions.) Denote by $\mathbf{x}_1$ and $\mathbf{x}_2$ the two ordinary contact points of the $A_1^2A_3$ sphere and by $\mathbf{x}_0$ the A_3 contact point. Let $\mathbf{e}_1$ denote the principal direction corresponding to the ridge, at $\mathbf{x}_0$. Then we require: (1) $\mathbf{e}_1$ is not in the plane of the three points $\mathbf{x}_0, \mathbf{x}_1, \mathbf{x}_2$, and (2) $\mathbf{x}_1$ and $\mathbf{x}_2$ are not in Ω, and the chord $\mathbf{x}_1\mathbf{x}_2$ is not parallel to Ω. In fact if $\mathbf{x}_1$ and $\mathbf{x}_2$ are on the same side of Ω then we get transition $A_1^2A_3$-I and otherwise we get $A_1^2A_3$-II.

7) The A_5 Transition: This transition is particularly interesting in that it is entirely *local* in nature. There is no interference between parts of the surface which are far from each other. The A_5 transition on ridges has been described in [6] and in [15, §7.2.8]. 'Before' this transition, a ridge has two *turning points* where the contact of the sphere of curvature rises from the usual A_3 to A_4. At a turning point—invisible on the medial axis since A_4 does not represent a minimum of distance—the ridge is tangent to the corresponding line of curvature. See Figure 22. The turning point also marks a change in the ridge from 'hyperbolic' to 'elliptic'. The contact between the sphere of curvature and the surface is A_3 for both types of ridge; the difference is as follows. At hyperbolic ridge points, the sphere of curvature intersects the surface locally in two intersecting curves; the center of this sphere contributes to the symmetry set but never to the medial axis. At an elliptic ridge point the sphere of curvature intersects the surface locally in a single point. If the sphere has no further intersection with the surface then its center is on the medial axis. If the sphere has ordinary tangency with the surface at one other point then its center is an A_1A_3 point.

At the moment of A_5 transition, the ridge becomes wholly elliptic or wholly hyperbolic nearby, and remains so 'after' the transition. When the ridge becomes wholly elliptic, then on the medial axis two ribs can combine into a single rib (A_3 curve). Before the transition they are connected on the medial axis by a short piece of A_1^3 curve, which shrinks to a point. This is simulated in Figure 23, which is based on a surface such as that shown in Figure 24, left; see Method 2 below for more details.

Remark 5.1 It is important to note that, at the moment when the surface has an A_5-contact sphere, reached through a generic 1-parameter family of surfaces, *there is no A_1^3 curve present.* This is only possible 'on one side' of the transition, as above.

In the 'opposite' case, it is two pieces of hyperbolic ridge which join together on the surface. Before they join, on the surface there is a short piece of elliptic ridge terminating in two A_4

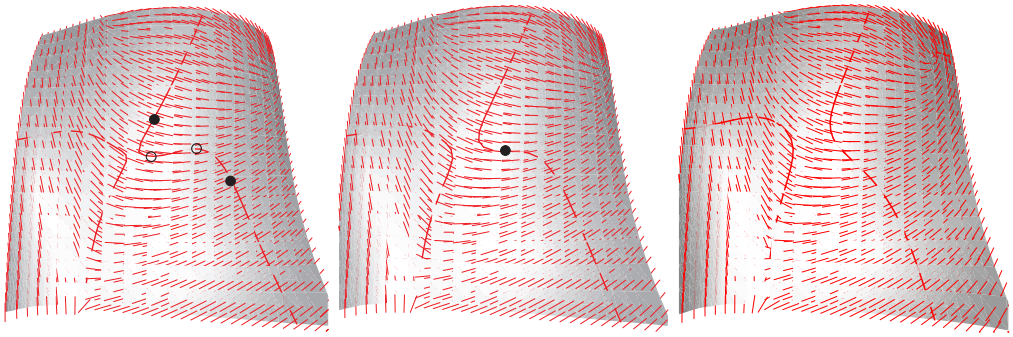

Figure 22: Ridges evolving through an A_5 transition, against a background of the corresponding principal direction field; the example is that of Equation (9). The ridge curve on the right of each figure is of interest: before the medial axis goes through the A_5 transition, the ridge curve loses two A_4 points (marked by open circles), that is points at which the ridge has a turning point and is tangent to the corresponding principal direction. The solid black dots are the contact points corresponding to the A_1A_3 points. Left, $t > 0$: there are two turning points, flanked by two A_1A_3 contact points; the part of the ridge between A_1A_3 contact points does not contribute at all to the medial axis. Center, $t = 0$: the ridge has degenerate tangency with the principal direction at $x = y = 0$, corresponding to the A_5 point. Both turning and A_1A_3 points have coalesced in this point, marked with a single black dot. Right, $t < 0$: there are no turning points (and no A_1A_3 contact points), and the whole ridge contributes to the medial axis. Note that if we run time backwards from the left figure, another ridge (left) is about to interact with the ridge of interest. This kind of interaction can never happen on the part of the ridge which contributes to the medial axis since turning points are involved. (Figure drawn with the SINGSURF package of Richard Morris.)

points. But this piece of elliptic ridge cannot contribute to the medial axis since it can be shown that it cannot contain the required A_1A_3 points. Without these, the A_3 curve cannot form part of the medial axis. (A full analysis of the symmetry set during an A_5 transition is given in [24]; see also [1, p.106].)

There are a number of ways of generating a surface where a sphere of curvature has A_5 contact and then perturbing it to give the transition. We shall describe two of these ways.

Method 1 Consider a surface S given locally in Monge form,

$$z = f(x, y) = a_0x^2 + a_2y^2 + b_0x^3 + b_1x^2y + b_2xy^2 + b_3y^3 + c_0x^4 + \ldots + d_0x^5 + \ldots + e_0x^6 + \ldots . \quad (6)$$

Thus the principal directions at the origin are along the x- and y-axes and the principal curvatures at the origin are $\kappa_1(0, 0) = 2a_0$, $\kappa_2(0, 0) = 2a_2$. We can assume that the origin is not an umbilic point on S, say $a_0 > a_2$, and also that $a_0 > 0$. To make the origin a ridge point corresponding to the first principal direction (that is, κ_1 has an extremum at the origin in the direction of the x-axis) we require $b_0 = 0$; the full conditions for an A_5 point at the origin are as follows (adapted and extended from [15]).

$$b_0 = 0, \quad c_0 = a_0^3 - \frac{b_1^2}{4(a_0 - a_2)}, \quad d_0 = -\frac{b_1c_1}{2(a_0 - a_2)} - \frac{b_1^2b_2}{4(a_0 - a_2)^2} \quad (7)$$

and three 'non-equalities'

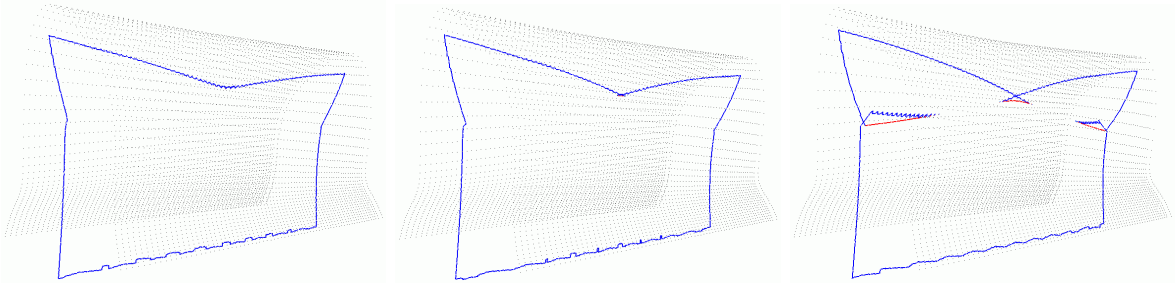

Figure 23: The A_5 transition. Right to left: in the upper part of each figure, two ribs on the medial axis of a surface such as that in Figure 24(a), initially connected by a short piece of A_1^3 curve, join together to form a continuous rib (A_3 curve). This is described as the collision of an A_3 curve and an A_1A_3 point in §3.2.5(d). The left to center transition is described as an invisible transition in §3.2.1.

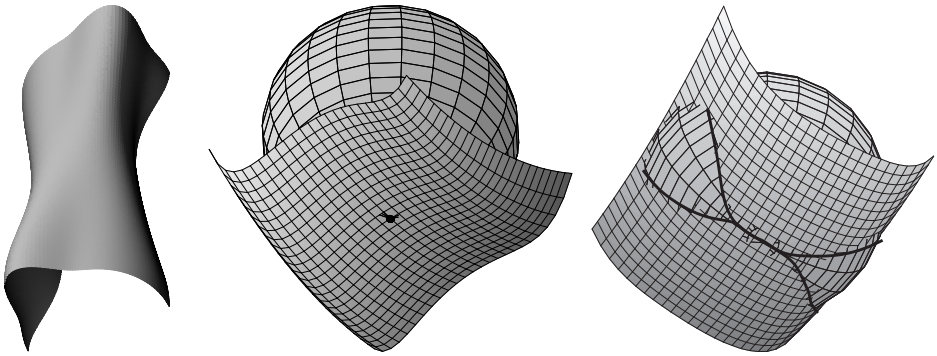

Figure 24: Left: a cylindrical surface with bumps of the kind used to produce the A_5 transition by Method 2. Right: two A_5 points, one where the intersection of the surface S and a sphere of curvature is isolated (left) and the other where the intersection consists of two curves having inflexional contact (drawn heavily). This is analogous to the situation at an ordinary (A_3) ridge point, where an elliptic ridge gives isolated intersection but a hyperbolic ridge gives an intersection with two *crossing* curves. The sphere on the right cannot be maximal, so that a hyperbolic ridge cannot contribute to the MA.

$$\begin{aligned} a_0 &\neq a_2 \quad \text{(not an umbilic point);} \\ (a_0-a_2)c_1 &\neq -b_1b_2 \quad \text{(the ridge needs to be a smooth curve)} \\ e_0 &\neq 2a_0^5 - \frac{c_1^2+2b_1d_1}{4(a_0-a_2)} + \frac{b_1(2a_0^3b_1-b_1c_2-2b_2c_1)}{4(a_0-a_2)^2} - \frac{b_1^2(2b_2^2+b_1b_3)}{8(a_0-a_2)^3} \\ &\quad \text{(the contact is not higher than } A_5\text{)} \end{aligned} \tag{8}$$

If (8) is changed to $e_0 < \ldots$ then the A_5 point is *elliptic*: the local intersection of S with the sphere of curvature of radius $1/\kappa_1$ is a single point. This means that the center lies on the medial axis so long as the sphere does not intersect S 'far away' from the origin. With $e_0 > \ldots$ in (8) the A_5 is *hyperbolic*, and the local intersection of S and its sphere of curvature is a pair of curves having inflexional contact at the origin. These two cases are illustrated in Figure 24, right.

Notes on genericity Let us assume that the sphere of curvature at a ridge point $\mathbf{p}$ has exactly A_5 contact with the surface. Then it can be shown [24] that for a family of surfaces to exhibit a generic A_5 transition we also require that *the line of curvature corresponding to the ridge does not have a torsion zero at* $\mathbf{p}$. This says that the osculating plane of this line of curvature has the normal (3-point) contact with the line of curvature at $\mathbf{p}$ and not higher contact.

As an example satisfying this condition we can take $z = f(x, y)$ where

$$f(x,y) = \tfrac{1}{2}x^2 + \tfrac{1}{8}y^2 + \tfrac{1}{2}x^2y + \tfrac{3}{10}xy^2 - \tfrac{1}{5}y^3 - \tfrac{1}{24}x^4 - \tfrac{2}{15}x^5 + \tfrac{283}{10800}x^6, \tag{9}$$

where we can add tx^4 to f to obtain our family of surfaces (the argument showing that this is a suitable monomial to add is in [24]). Figure 22 shows the ridges of this surface against a background of the principal direction field, whose integral curves are the lines of curvature.

Method 2 For illustrating the transition we start with a cylindrical surface having two long bumps and merge them into one. We construct a surface parametrized in cylindrical polar coordinates by θ and z: let

$$\rho := \rho_0 + \rho_0\, c_1\, \exp\left(-\frac{0.5\,(\theta-\theta_1)^2}{((1-\frac{z}{l})\,k_1 + \frac{z}{l}\,k_2)^2}\right) + \rho_0\, c_2\, \exp\left(-\frac{0.5\,(\theta-\theta_2)^2}{(\frac{z\,k_1}{l} + (1-\frac{z}{l})\,k_2)^2}\right) \tag{10}$$

so that the surface has parametrization $(\rho\cos\theta, \rho\sin\theta, z)$. The idea is that there will be two bumps, centered on $\theta = \theta_1, \theta_2$, and between $z = 0$ and $z = l$ one bump diminishes and the other increases in spread. The constants $\rho_0,\ c_1,\ c_2,\ k_1,\ k_2$ govern the radius of the cylinder, the size of the bumps and their spread. A typical such surface is shown in Figure 24, left.

For the example used to produce Figure 23, the following values were taken: $3 \le z \le 7,\ \theta_1 = 1.3, \theta_2 = 1.7$ (both in radians), $k_1 = 0.1,\ k_2$ from 0.33 to 0.38. The formation of a segment of A_1^3 curve can be seen between the two pieces of A_3 curve on the medial axis.

6 Conclusions

We have investigated the instabilities of the medial axis from a geometrical viewpoint. We have shown that these instabilities or transitions arise in several ways. A contact point with a sphere can acquire an additional degree of contact, giving an *invisible transition*, in which case the topology of the medial axis does not change. Alternatively the medial axis experiences a self-intersection, which does change the topology of the medial axis; these are the various *collision of singularity transitions*. First, we demonstrated that there are only *three* generic invisible transitions, $A_1^2 \to A_1A_3$, $A_1^3 \to A_1^2A_3$, and $A_3 \to A_5$. Second, we have shown that

collisions within the medial axis can only occur between points and curves (point-point, point-curve, curve-curve), not involving sheets (point-sheet, curve-sheet, sheet-sheet), and that there are *eleven* such cases. Altogether, these fourteen cases enumerate the two directions for each of seven types of transitions in both direction that can generically occur in a one-parameter family of perturbations, a result consistent with Bogaevsky's work. [5]

References

[1] V. I. Arnold, V. V. Goryunov, O. Lyashko, and V. A. Vasil'ev. *Singularity Theory II*, volume 39. Springer-Verlag, 1993.

[2] I. A. Bogaevsky. Metamorphoses of singularities of minimum functions, and bifurcations of shock waves of the Burgers Equation with vanishing viscosity. *St Petersburg (Leningrad) Math. J.*, 1:807–823, 1990.

[3] I. A. Bogaevsky. Perestroikas of shocks and singularities of minimum functions. *Physica D*, 173:1–28, 2002.

[4] J. W. Bruce and P. J. Giblin. Growth, motion and 1-parameter families of symmetry sets. *Proceedings of the Royal Society of Edinburgh*, 104A:179–204, 1986.

[5] J. W. Bruce and P. J. Giblin. *Curves and Singularities*. Cambridge University Press, 2nd edition, 1992.

[6] J. W. Bruce, P. J. Giblin, and F. Tari. Ridges, crests and sub-parabolic lines of evolving surfaces. *IJCV*, 18(3):195–210, June 1996.

[7] M.-C. Chang and B. B. Kimia. Regularizing 3D medial axis using medial scaffold transforms. In *CVPR'08*, page Submitted. IEEE Computer Society, 2008.

[8] M.-C. Chang, F. F. Leymarie, and B. B. Kimia. 3D shape registration using regularized medial scaffolds. In *Proceedings of the 3D Data Processing, Visualization, and Transmission (3DPVT)*, pages 987–994, Washington, DC, USA, September 2004. IEEE Computer Society.

[9] J. Damon. Determining the geometry of boundaries of objects from medial data. *Int. J. Comput. Vision*, 63(1):45–64, 2005.

[10] J. Damon. Tree structure for contractible regions in $\mathbf{R}^3$. *Int. J. Comput. Vision*, 74(2):103–116, 2007.

[11] P. J. Giblin and B. B. Kimia. On the local form of symmetry sets, and medial axes, and shocks in 3D. In *Proceedings of the IEEE Computer Society Conference on Computer Vision and Pattern Recognition*, pages 566–573, Hilton Head Island, South Carolina, USA, June 13-15 2000. IEEE Computer Society Press.

[12] P. J. Giblin and B. B. Kimia. Transitions of the 3D medial axis under a one-parameter family of deformations. In *ECCV'02*, volume 2350 of *Lecture Notes in Computer Science*, pages 718–724. Springer, 2002.

[13] P. J. Giblin and B. B. Kimia. On the local form and transitions of symmetry sets, medial axes, and shocks. *IJCV*, 54(Issue 1-3):143–157, August 2003.

[5] **Acknowledgments:** We gratefully acknowledge the support of NSF grants BCS-9980091 and ECS-0070887. The first author also acknowledges the European Union for the grant DSSCV and the first and third authors acknowledge a grant from the EPSRC. The simulations were performed by Frederic Leymarie and Ming-Ching Chang using a numerical simulation originally developed in [20] and later extended by Ming-Ching Chang. We also appreciate the assistance of Mireille Boutin, Raghavan Dhandapani and Declan Davis in creating some example cases and of Ming-Ching Chang in the final editing of the paper.

[14] P. J. Giblin and B. B. Kimia. A formal classification of 3D medial axis points and their local geometry. *PAMI*, 26(2):238–251, February 2004.

[15] P. L. Hallinan, G. G. Gordon, A. L. Yuille, P. J. Giblin, and D. Mumford. *Two and three dimensional patterns of the face*. A.K. Peters, Natick, Massachusetts, 1999.

[16] M. S. Johannes, T. B. Sebastian, H. Tek, and B. B. Kimia. Perceptual organization as object recognition divided by two. In *Workshop on Perceptual Organization in Computer Vision*, pages 41–46, 2001.

[17] P. Klein, T. Sebastian, and B. Kimia. Shape matching using edit-distance: an implementation. In *Twelfth Annual ACM-SIAM Symposium on Discrete Algorithms (SODA)*, pages 781–790, Washington, D.C., January 7-9 2001.

[18] P. Klein, S. Tirthapura, D. Sharvit, and B. Kimia. A tree-edit distance algorithm for comparing simple, closed shapes. In *Tenth Annual ACM-SIAM Symposium on Discrete Algorithms (SODA)*, pages 696–704, San Francisco, California, January 9-11 2000.

[19] L. Lam, S.-W. Lee, and C. Y. Suen. Thinning methodologies-a comprehensive survey. *IEEE Trans. on PAMI*, 14(9):869–885, September 1992.

[20] F. F. Leymarie. *3D Shape Representation via Shock Flows*. PhD thesis, Division of Engineering, Brown University, Providence, RI, 02912, May 2003.

[21] F. F. Leymarie, P. J. Giblin, and B. B. Kimia. Towards surface regularization via medial axis transitions. In *Proceedings of International Conference on Pattern Recognition*, volume 3, pages 123–126, Cambridge, England, August 2004. Computer Society Press.

[22] F. F. Leymarie and B. B. Kimia. From the infinitely large to the infinitely small: Applications of medial symmetry representations of shape. In K. Siddiqi and S. Pizer, editors, *Medial Representations: Mathematics, Algorithms and Applications*, page In Press. Kluwer Academic Publishers, 2007.

[23] R. L. Ogniewicz and O. Kubler. Hierarchic voronoi skeletons. *Pattern Recognition*, 28(3):343–359, 1995.

[24] A. J. Pollitt. *Euclidean and Affine Symmetry Sets and Medial Axes*. PhD thesis, University of Liverpool, 2004. http://www.liv.ac.uk/∼pjgiblin/.

[25] T. Sebastian, P. Klein, and B. Kimia. Recognition of shapes by editing their shock graphs. *PAMI*, 26:551–571, May 2004.

[26] D. Shaked and A. M. Bruckstein. Pruning medial axes. *Computer Vision and Image Understanding*, 69:156–169, 1998. 2.

[27] A. Tamrakar and B. B. Kimia. Medial visual fragments as an intermediate image representation for segmentation and perceptual grouping. In *Proceedings of CVPR Workshop on Perceptual Organization in Computer Vision*, page 47, 2004.

[28] S. Tari and J. Shah. Extraction of shape skeletons from grayscale images. *Computer Vision Image Understanding*, 66(2):133–146, 1997.

[29] H. Tek and B. B. Kimia. Boundary smoothing via symmetry transforms. *JMIV*, 14(3):211–223, May 2001.

[30] N. Trinh and B. B. Kimia. A symmetry-based generative model for shape. In *ICCV '07: Proceedings of the Eleventh IEEE International Conference on Computer Vision*, Rio de Janeiro, Brazil, October 2007. IEEE Computer Society.